GEORGIA INSTITUTE OF TECHNOLOGY — OFFICE OF CONTRACT ADMINISTRATION

PROJECT ADMINISTRATION DATA SHEET

[x] ORIGINAL [ ] REVISION NO. ______

Project No. A-3195 — DATE 3/22/82

Project Director: ~~Dr. D. J. Kozakoff~~ Mr. Joe M. Newton — School/Lab EML/RSD

Sponsor: U. S. Army Missile Command; Redstone Arsenal, AL 35898

Type Agreement: Delivery Order No. 0042 under No. DAAH01-81-D-A003

Award Period: From 3/12/82 To 9/30/82 (Performance) ______ (Reports)

Sponsor Amount: $30,173.90 — Contracted through:

Cost Sharing: None — GTRI/~~GIT~~

Title: Radome Computer Analysis Methodology RDF-43

ADMINISTRATIVE DATA

OCA Contact Linda H. Bowman x4820

1) Sponsor Technical Contact:

Dr. M. M. Hallum
Systems Simulation & Development Directorate
U. S. Army Missile Command
Attn: DRSMI-RDF
Redstone Arsenal, AL 35898
205-876-4141

2) Sponsor Admin/Contractual Matters:

Mr. Thomas A. Bryant
ONR Resident Rep.
GIT
207 O'Keefe Bldg
Atlanta, GA 30332

Defense Priority Rating: DO-A2 under DMS Reg. 1 — Security Classification: unclassified

RESTRICTIONS

See Attached government Supplemental Information Sheet for Additional Requirements.

Travel: Foreign travel must have prior approval – Contact OCA in each case. Domestic travel requires sponsor approval where total will exceed greater of $500 or 125% of approved proposal budget category.

Equipment: Title vests with government; except that items costing less than $1,000 vests with GIT if prior approval to purchase is obtained from the Contracting Officer.

COMMENTS:

MAR 1982
RECEIVED
Research Reports
Office

COPIES TO:

Administrative Coordinator	Research Security Services	EES Public Relations (2)
Research Property Management	Reports Coordinator (OCA) ✓	Computer Input
Accounting	Legal Services (OCA)	Project File
Procurement/EES Supply Services	Library	Other ______

FORM OCA 4:781

GEORGIA INSTITUTE OF TECHNOLOGY OFFICE OF CONTRACT ADMINISTRATION

SPONSORED PROJECT TERMINATION SHEET

2-5R-321

Date 9/30/82

Project Title: Radome Computer Analysis Methodology RDF-43

Project No: A-3195

Project Director: Dr. D. J. Kozakoff

Sponsor: US Army Missile Command; Redstone Arsenal, AL

Effective Termination Date: 9/30/82

Clearance of Accounting Charges: 11/30/82

Grant/Contract Closeout Actions Remaining:

- [x] Final Invoice ~~and Closing Documents~~
- [ ] Final Fiscal Report
- [x] Final Report of Inventions
- [x] Govt. Property Inventory & Related Certificate
- [ ] Classified Material Certificate
- [ ] Other ______________________

Assigned to: EML ~~(School~~/Laboratory)

COPIES TO:

Administrative Coordinator
Research Property Management
Accounting
Procurement/EES Supply Services
Research Security Services
Reports Coordinator (OCA)
Legal Services (OCA)
Library
EES Public Relations (2)
Computer Input
Project File
Other ______________

FORM

A-3195

Technical Report #1
and
Cost and Performance Report #1

Report Period
1 March 1982 through 31 March 1982

RADOME COMPUTER ANALYSIS METHODOLOGY

D. J. Kozakoff

Contract No. DAAH01-81-D-A003
Delivery Order 0042
EES Project A-3195

Effective Date: 3/12/82
Expiration Date: 9/30/82

Prepared for

U.S. Army Missile Command
Redstone Arsenal, AL 35898
Attn: DRSMI-RDF

Prepared by

Engineering Experiment Station
Georgia Institute of Technology
Atlanta, GA 30332

WORK PERFORMED IN THIS REPORTING PERIOD

This project was initiated in this reporting period. The only work accomplished were telecons and planning sessions with the contract technical monitor.

PROBLEMS ENCOUNTERED IN THIS REPORTING PERIOD

None

WORK PLANNED FOR THE NEXT REPORTING PERIOD

A project kick-off meeting in Atlanta will be held to quantify the goals and plan of attack in accomplishing this study.

A-3195

Cost Information

The following charges have been incurred against the contract during period 12 March through 31 March, 1982

	Expended	Encumbered
Personal Services (PS)	$240.75	
Materials and Supplies	0	
Travel	0	-NONE-
Overhead (@ 55% of PS)	147.76	
Retirement (@ 11.59% of PS)	27.90	
TOTAL	$416.41	

The breakdown of personal services is as follows:

	Dollars	Approximate Man Hours
Principal Research Scientists/Engineers	0	0
Senior Research Scientists/Engineers	240.75	11
Research Scientists II/Engineers II	0	0
Research Scientists I/Engineers I	0	0
Technicians/Draftsmen	0	0
Students	0	0
Secretarial/Clerical/Other	0	0
TOTAL	$240.75	11

The current financial status of the contract is as follows:

	Budget As Proposed	Expended	Free Balance
Personal Services (PS)	$11,620.22	$240.75	$11,379.47
Materials and Supplies	600.00	0	600.00
Travel and Shipping	900.00	0	900.00
Computer	5,000.00	0	5,000.00
Overhead	10,706.90	147.76	10,559.14
Retirement	1,346.78	27.90	1,318.88
[illegible]	$30,173.90	$416.41	$29,757.49

FUNDING

Based on present full funding, the funding and equivalent man hours are sufficient to complete the task. Approximately 1.4% of the proposed task has been completed.

A-3195

Technical Report #2
and
Cost and Performance Report #2

Report Period

1 April through 31 July 1982

RADOME COMPUTER ANALYSIS METHODOLOGY

D. J. Kozakoff

Contract No. DAAH01-81-D-A003
Delivery Order 0042
EES Project A-3195

Effective Date: 3/12/82
Expiration Date: 9/30/82

Prepared for

U.S. Army Missile Command
Redstone Arsenal, AL 35898
Attn: DRSMI-RDF

Prepared by

Engineering Experiment Station
Georgia Institute of Technology
Atlanta, Georgia 30332

WORK PERFORMED IN THIS REPORTING PERIOD

Complete radome modeling was accomplished to assess the affects of backwall and bulkhead reflections and antenna scattered energy. In addition, the flat panel wall transmission subroutine was scrutinized via comparison of measured and predicted data. The results show the predictions are larger insertion phase values than measured at MICOM.

Various trips were made to interface with the MICOM Technical Contract Monitor.

PROBLEMS ENCOUNTERED IN THIS REPORTING PERIOD

None.

WORK PLANNED FOR NEXT REPORTING PERIOD

The final written report should be completed and a rough draft will be delivered to MICOM for review.

Cost Information

The following charges have been incurred against the contract during period July 1 - July 31, 1982

	Expended	Encumbered
Personal Services (PS)	1,077.09	-0-
Materials and Supplies	4.50	-0-
Travel	202.10	-0-
Overhead (@ 73% of PS)	757.87	-0-
Retirement (@ 11.11% of PS)	190.50	-0-
TOTAL	2,232.06	-0-

The breakdown of personal services is as follows:

	Dollars	Approximate Man Hours
Principal Research Scientists/Engineers		
Senior Research Scientists/Engineers	882.75	39
Research Scientists II/Engineers II		
Research Scientists I/Engineers I		
Technicians/Draftsmen		
Students Secretarial/Clerical/Other	194.34	28
TOTAL	1,077.09	67

The current financial status of the contract is as follows:

	Budget As Proposed	Expended	Free Balance
Personal Services (PS)	11,620.22	13,084.89	(1,464.67)
Materials and Supplies	600.00	176.48	432.52
Travel and Shipping	900.00	514.03	385.97
Computer	5,000.00	267.54	4,732.46
Overhead	10,706.90	8,344.50	2,367.40
Fringe Benefits	1,346.78	1,356.58	(9.80)
Encumbered	-0-	-0-	-0-
FUNDING	30,173.90	23,744.02	6,429.88

Based on present full funding, the funding and equivalent man hours are sufficient to complete the task. Approximately 79 % of the proposed task has been completed.

A-3195

FINAL TECHNICAL REPORT

Project A-3195

RADOME COMPUTER ANALYSIS METHODOLOGY

September 1982

D. J. Kozakoff

and

D. Bagwell

Contract No. DAAH01-81-D-A003

Delivery Order 0042

Prepared for

U. S. ARMY MISSILE COMMAND
Redstone Arsenal, AL 35898
Attn: DRSMI-RDF

Prepared by

Engineering Experiment Station
Georgia Institute of Technology
Atlanta, Georgia 30332

UNCLASSIFIED

SECURITY CLASSIFICATION OF THIS PAGE (When Data Entered)

REPORT DOCUMENTATION PAGE

READ INSTRUCTIONS BEFORE COMPLETING FORM

1. REPORT NUMBER	2. GOVT ACCESSION NO.
3. RECIPIENT'S CATALOG NUMBER	
4. TITLE (and Subtitle) RADOME COMPUTER ANALYSIS METHODOLOGY	5. TYPE OF REPORT & PERIOD COVERED Final Report 3/12 - 9/30/82
	6. PERFORMING ORG. REPORT NUMBER
7. AUTHOR(s) D. J. Kozakoff, D. Bagwell	8. CONTRACT OR GRANT NUMBER(s) DAAH01-81-D-A003 Delivery Order 0042
9. PERFORMING ORGANIZATION NAME AND ADDRESS Engineering Experiment Station, Georgia Institute of Technology, Atlanta, Georgia 30332	10. PROGRAM ELEMENT, PROJECT, TASK AREA & WORK UNIT NUMBERS
11. CONTROLLING OFFICE NAME AND ADDRESS U. S. Army Missile Command, Redstone Arsenal, Alabama 35898, Project Monitor: K. Letson	12. REPORT DATE September 1982
	13. NUMBER OF PAGES
14. MONITORING AGENCY NAME & ADDRESS (if different from Controlling Office)	15. SECURITY CLASS. (of this report) UNCLASSIFIED
	15a. DECLASSIFICATION/DOWNGRADING SCHEDULE

16. DISTRIBUTION STATEMENT (of this Report)

17. DISTRIBUTION STATEMENT (of the abstract entered in Block 20, if different from Report)

18. SUPPLEMENTARY NOTES The views and conclusions contained in this document are those of the authors and should not be interpreted as necessarily representing the official policies, either expressed or implied, of the U. S. Army Missile Command.

19. KEY WORDS (Continue on reverse side if necessary and identify by block number)

Radome Analysis, Computer Methodology, Boresight Errors.

20. ABSTRACT (Continue on reverse side if necessary and identify by block number)

This document contains an assessment of the accuracy of a three-dimensional backward ray trace computer code when various parameters are factored into the mathematics. This includes backwall and bulkhead reflections. Predictions are compared to measured data for a test case.

TABLE OF CONTENTS

1.0 INTRODUCTION

This document summarizes a study with an objective of quantifying prediction errors in various computerized radome analyses techniques. In an earlier study [1], the various analysis methods including forward and backward ray trace, surface integration and plane wave spectra were investigated. It was determined that for antennas greater than approximately five wavelengths in diameter, the three-dimensional backward ray trace offered potential for superior accuracy while maintaining reasonable operating cost relative to the surface integration or plane wave spectra approaches which could cost up to $10 per data point in computer cost (i.e. one look angle and one frequency).

Of the computer code survey completed in the first study, the three most viable which were selected for study were the Georgia Tech three-dimensional backward ray trace, and RADEP3 codes and the Auburn University code. All these are backward ray trace formulations; a comparative summary of modeling features are given in Table 1-1. The tradeoffs in analysis method performance results appear in Table 1-2.

In this study, the preferred Georgia Tech code was modified in detail to model additional error contributors which were believed to be the major error sources between theoretical predictions and actual results. In addition, the wall transmissions subroutine was exercised for an example and compared with actual measurements (performed as part of this program) to determine the validity of the theory. Finally, the program was exercised for a particular radome problem and the results compared to actual measurements to determine if prediction improvement could be obtained with the modeling modifications.

Table 1-1

COMPARISON OF SELECTED COMPUTER CODES

Program	Bulkhead Reflections	Backwall Reflections	Radome Tip Modeling	Radome Wall Taper	Arbitrary Circular Polarization	Circumferential Wall Variations	Antenna Scattering	Multilayer Walls
Georgia Tech	No	No	Yes	Yes	Yes	Yes	No	Yes
Auburn University	No	Yes	Yes	No	No	No	No	Yes
RADEP3	No	No	Yes	Yes	No	No	No	Yes

Table 1-2

TRADEOFF OF ANALYSIS METHODS

	Operating Cost	BSE Accuracy	Sidelobe Predictor Accuracy	Machine Size Required
Ray Trace Transmit	Low	Good	Poor	Small
Ray Trace Receive	Low	Good	Good	Small
PWS	High	Good	Good	Large
Surface Integration	Extremely High	Excellent	Good	Very Large

2.0 OVERVIEW OF SELECTED RADOME ANALYSIS METHOD

A flow chart of the ray trace program used herein is shown in Figure 2-1. The program interactively asks the user to input the necessary parameters to describe the (tangent ogive) radome, the antenna, and the incoming wave polarization. The program is currently preselected to the principal planes (El = 0 and AZ = 0) from 0 to 30 degrees in increments of 1 degrees. The antenna sample spacing is selected by the user. A ray is then traced outward from each sample point in the direction of the incoming wavefront. The intersection of each ray with the radome is then found by a modified regula falsi root solving method. The normal to the tangent ogive at the intersection is found and used along with the direction of propagation to define the plane of incidence. The electric field is then broken into components perpendicular and parallel to the plane of incidence. The transmission and IPD are then calculated for both of the above cases, the radome wall being assumed to be locally flat at the intercept point. The subroutine that calculates the affect of the wall takes into account multi-layer sandwiches and multiple reflections within the radome wall (see Section 5).

The electric field is then reflected in terms of the original azimuth and elevation directions for numerical integration (summation) at the antenna aperture. Monopulse sum and difference illuminations are used in sequence to allow computation of standard monopulse error voltages and to thus derive a measure of boresight error in both the elevation and azimuth channels. The ray trace technique is illustrated in Figure 2-2.

The specific subroutines that compute the affects of bulkhead, backwall and internal antenna reflections are described in detail in subsequent sections of this report.

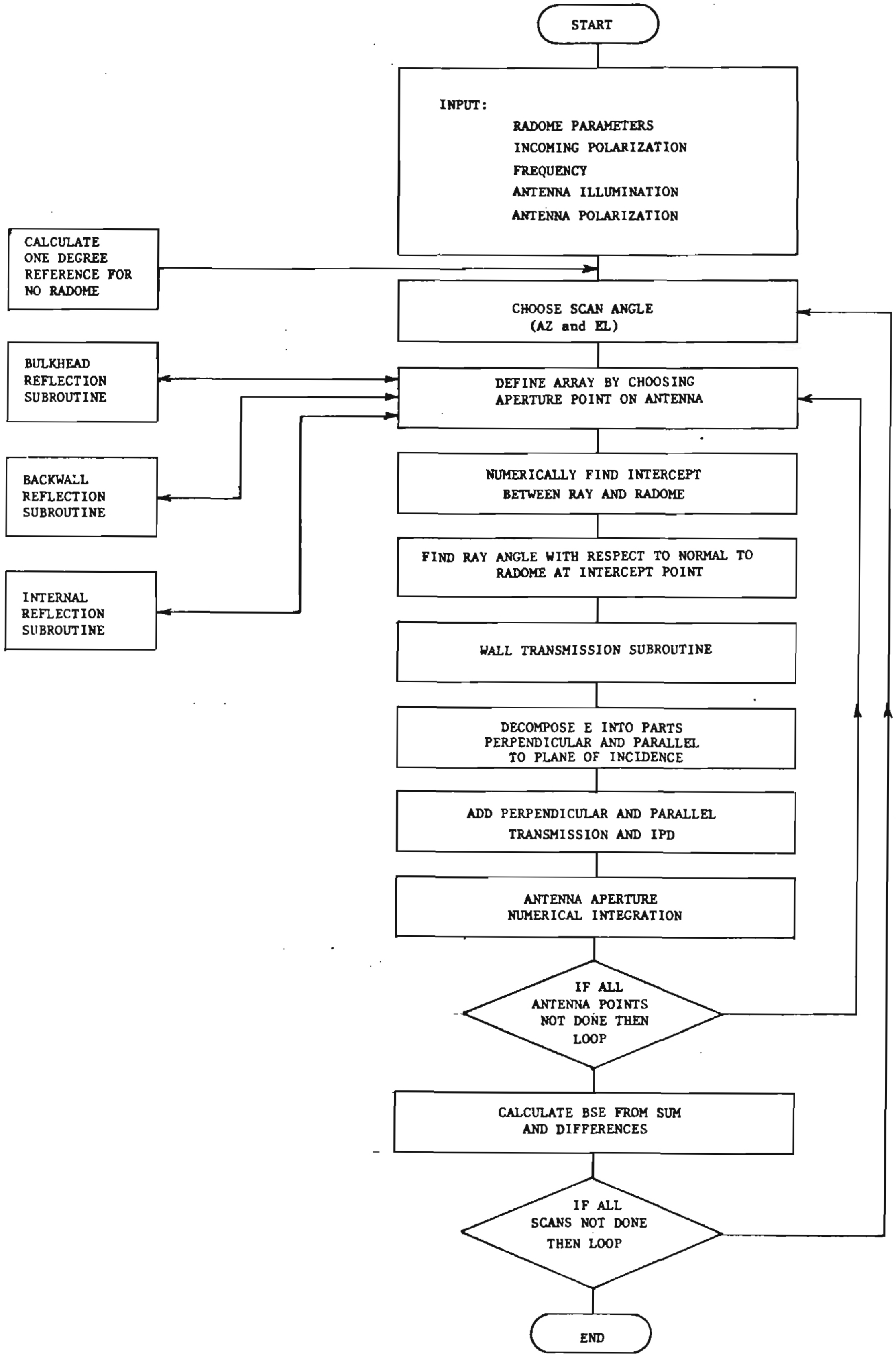

Figure 2-1. Program Flow Chart

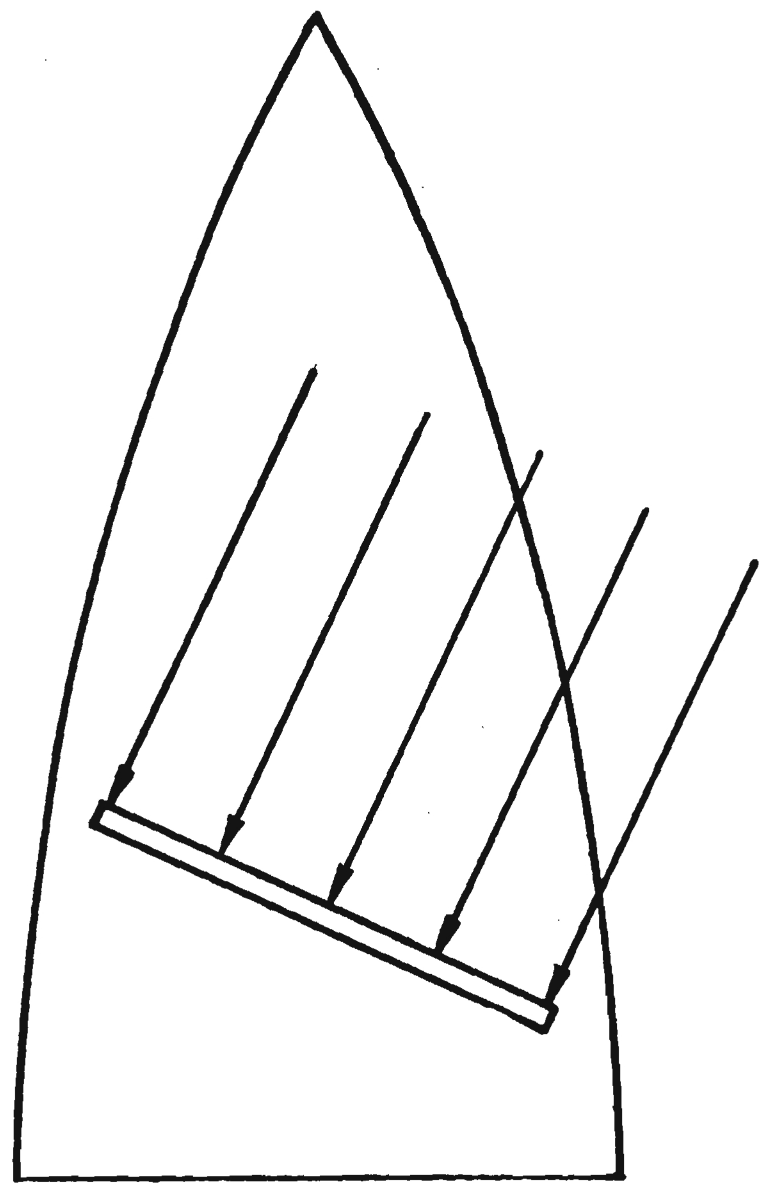

Figure 2-2. Backward Ray Trace Method.

3.0 DISCUSSION OF ANALYSIS ERRORS

3.1 General

The extent that the sidewall and bulkhead reflections and antenna scattered energy can affect boresight error calculations is highly dependent upon the properties of the radome and the antenna that it encloses. A radome can be theoretically designed so that reflections have negligible affects on the boresight error, but in practice, the reflections usually are large enough to influence the boresight errors.

The effect of bulkhead reflections depend mainly on the backlobe properties of the antenna. The magnitude of rays reflecting off the rear bulkhead plate are approximately the same as those directly striking the antenna. If the antenna is located close to the bulkhead then the area on the bulkhead for rays to reflect and strike the antenna is restricted and the extent of bulkhead reflections decrease.

Generally, bulkhead reflections will not have much affect until the angle of incidence of the incoming rays (with respect to the radome axis) become larger. Our antenna model assumes that the rear pattern is a mirror image of the forward pattern, decreased in magnitude by a user specified number of decibels (generally 20 dB). This should reasonably be a good model for a variety of antennas. In actual applications, positioners and electronic gear may block some of the reflections from reaching the antenna. As the incidence angle of the incoming rays gets much greater than 45 degrees, the bulkhead reflections cannot hit the antenna since they become parallel to the plane of the antenna.

The reflections off the radome side walls is another parameter that can affect boresight errors. The reflectance of a design wall may only be one percent for the electric field (.01% for the power) for a well-designed radome. In practice, erosion and ablation may change the thickness and heating may change the electrical properties of the wall. Reflectances may then get very large, potentially even being larger than fifty percent. The sidewall reflections strike only a small segment of the antenna. As radome wall reflectances become large, the boresight errors may become very large as a result of this concentration of reflected energy. The size and position of the antenna also has an effect on sidewall reflections.

A limiting incidence angle exists, below which no sidewall reflections can occur (see Section 3.2). As the size of the antenna approaches that of the radome immediately surrounding it, this limiting angle goes to 0. As the size of an antenna increases, the effects of sidewall reflections will increase regardless of incidence angle (as long as the incidence angle is larger than the limiting angle).

The fineness ratio of the radome also has an effect on sidewall reflections, since the position and angle of the radome wall at the reflection point determines where the reflected rays can strike the antenna. A large fineness ratio should lead to increased sidewall reflections, as should moving the antenna towards the base of the radome. Sidewall affects would be expected to increase if the antenna were not perpendicular to the incident radiation.

The effects of antenna scattered energy on boresight error calculations are highly dependent upon the reflectance of the radome walls. Some of these rays may reflect off the radome wall twice before striking the antenna, enhancing the need for high reflectance to get measureable effects. The properties of the antenna control how much of the scattered energy is absorbed. A large antenna increases the probability that a reflecting ray can hit the antenna. The antenna's illumination function determines how much of the incident rays energy is scattered and the distribution of this scattered energy. A low fineness ratio for the radome should allow more rays to hit the antenna with fewer sidewall reflections. Antenna scattered energy should not be as important in typical radomes as the other types of reflections, because the reflected energy is distributed fairly evenly over the antenna aperture, reducing its affect on boresight error calculations.

3.2 Sidewall Reflections

Part of the energy incident on an antenna enclosed in a radome consists of rays that transmit through the radome, hits another position of the radome where some of the energy is reflected back into the antenna (or misses the antenna and is reflected again). The rays that reflect off the radome wall only once before striking the antenna are the only ones that are considered herein. Higher order reflections can be ignored for typical radomes since the amount of energy reflected at each contact with the radome wall becomes insignificant.

The amount of energy that is reflected off a radome wall is dependent on the angle of the incoming rays. To develop the analyses we define the antenna reference plane to be the plane of the antenna when the antenna is looking down the axis of the radome illustrated in Figure 3-1. At some incidence angle part of the incident wave that would normally hit the antenna reference plane outside of the radome is unable to hit this plane because it has already been reflected by the radome. The radome casts a "shadow" on the antenna reference plane.

The energy absent from this shadow region is that which will be reflected off the radome wall. A limiting angle of incidence with respect to the radome axis exists, below this limit no shadow will be cast and no energy can be reflected. This angle is found to be

$$\theta_{lim} = \tan^{-1}\left(\frac{D'/2}{L-\Delta}\right) \tag{3-1}$$

An array of sample points is set up inside any shadow that is cast. The sample point spacing is selected according to the sample point spacing used on the antenna in the standard ray-tracing method.

A ray incident on the shadow intercepts the radome in two locations. These locations are found numerically using the same techniques as the standard ray-trace. The energy striking the antenna must be transmitted at the first intercept and reflected at the second. The effects on the magnitude and phase of the incoming ray by the transmission and reflection are calculated using the model described in

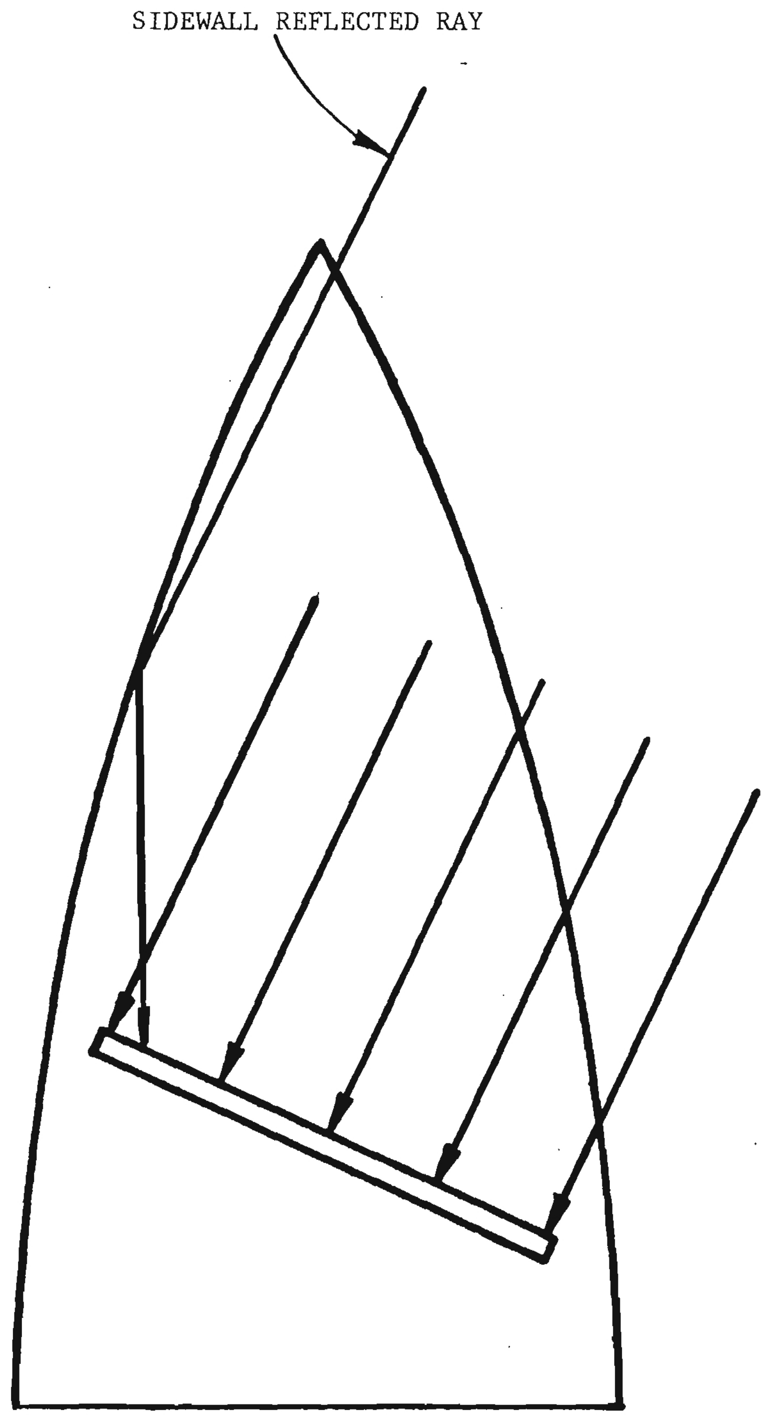

Figure 3-1. Sidewall Reflection Component Added to Ray Trace.

Section 5. The direction vector C of the reflected ray is:

$$C = K - (K \cdot N) N \tag{3-2}$$

The coordinates of the point where the reflected ray intersects the antenna aperture must be found for all reflected rays that will hit the antenna. The equation for the rotated antenna's aperture plane is obtained by inverting the rotation matrix that rotated the antenna to its position and solving for the points X'=0 which are contained in the aperture plane. (See Appendix C for details). The intersection point can now be found by solving the equations for the antenna plane with those describing the vector C.

A phase shift is added to the electric field at the antenna due to the longer path that the reflected ray must take with respect to a reference ray coming directly in. The magnitude of the electric field absorbed by the antenna is decreased for fields not in the plane (direction vector normal to the plane) of the antenna. After these two effects on the electric field are accounted for, the electric field is added to the computer model of the monopulse network in the same method as direct incidence rays.

3.3 Bulkhead Reflections

Many missiles have a bulkhead plate between the radome of the missile body. If the bulkhead is not absorber treated, then incoming electromagnetic rays can reflect off this plate and strike the backside of the antenna; these rays are capable of causing boresight errors.

The analysis treats the reflections off the bulkhead plate as if it were flat, perfectly conducting, and located at the origin of the radome coordinates. This should be a fairly accurate model for many missiles.

The antenna is modeled the same as in the standard ray-trace, i.e., the same samples point definitions are used. However, the rays incident on the back of the antenna are reduced in gain. The user corrects for this in the program by inputing the rear antenna gain factor. This factor can also include any losses which come from imperfect reflection off of the bulkhead.

Mathematics

The rays are traced from the antenna sample points to the plane of the bulkhead separation plate along the vector $(-K_x, K_y, K_z)$ illustrated in Figure 3-2. (Direction vector for incident rays is K_x, K_y, K_z. The vector $(-K_x, K_y, K_z)$ was chosen because it will become the direction vector $\overline{K}$ after reflection off of the plate. Any rays that pierce the side of the radome before hitting the bulkhead plate are discarded since they are not reflected by the bulkhead. The rays are then traced along the direction vector $\overline{K}$ to the plane of the antenna. The intersection between the plane and ray is found by inverting the rotation matrix as described in Section 3.2. If this ray hits the antenna itself then it is discarded because rays directly incident on the antenna have already been treated in the standard ray-trace. The rays are then ray traced from the antenna plane through the radome wall along the direction $\overline{K}$ in the same manner as the standard ray-trace.

The remaining rays may be thought of as being incident at the radome, reflecting off the bulkhead, then striking the antenna. The magnitude of the electric field is adjusted to account for non-normal incidence on the antenna as described in Section 3.2. The phase of the

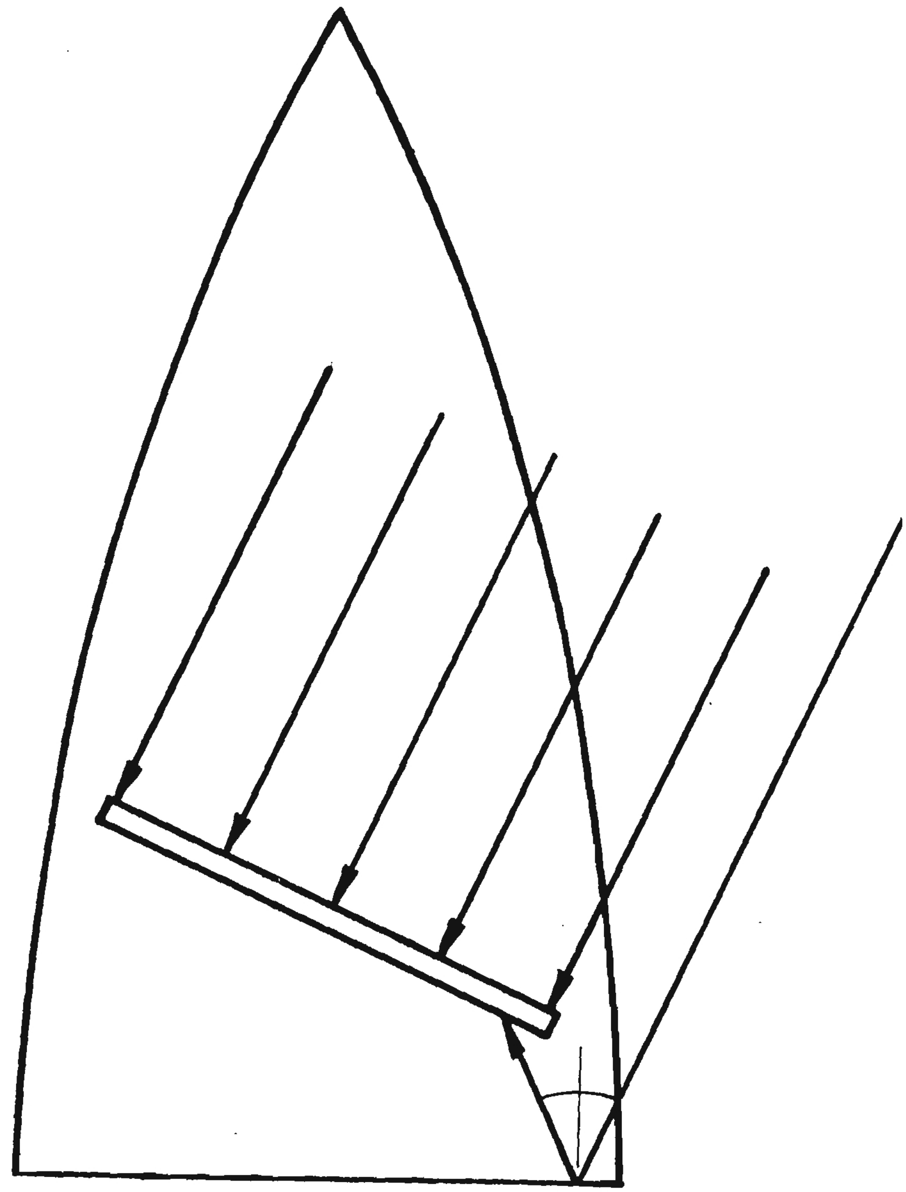

Figure 3-2. Bulkhead Reflection Added to Backward Ray Trace.

electric field is adjusted to allow for the additional path from the antenna to the bulkhead to the antenna plane. The electric field is then summed to the monopulse model at the sample point on the antenna.

3.4 Antenna Scattered Energy

Not all of the energy striking an antenna is absorbed by the antenna. The energy absorbed by an antenna is dependent on the antenna's illumination function. An approximation to the energy reflected by the antenna is the inverse of the illumination functions.

The antenna scattered energy can bounce off the radome wall one or more times before striking the antenna. At each reflection most of the energy is transmitted through the radome wall if the radome is well designed. Our model takes into account one and two reflections off the radome, ignoring rays that miss the antenna after 2 radome wall reflections.

Mathematics

The standard ray-tracing method is used to trace the rays through the radome wall to the antenna, including use of the same sample points. At the antenna the rays are multiplied by the illumination function inverse being evaluated at the sample point. The antenna is assumed to be flat, because of this the rays reflecting off the antenna will intersect the radome wall at the same place that the ray initially entered the radome (see Figure 3-3). At the reflection point the direction of the ray is changed and the magnitude and phase of the electric field are changed using the same techniques as the sidewall reflections described in Section 3.2. The ray is then tested to see if it will intersect the antenna, go through the base of the radome, or strike the radome wall in another location.

If the ray intersects the antenna the intersection point is found, the electric fields magnitude and phase are adjusted, and the electric field is summed to the monopulse model, all of these being done in the same manner as the sidewall reflections of Section 3.2. If the ray passes through the base of the radome without intersecting the antenna

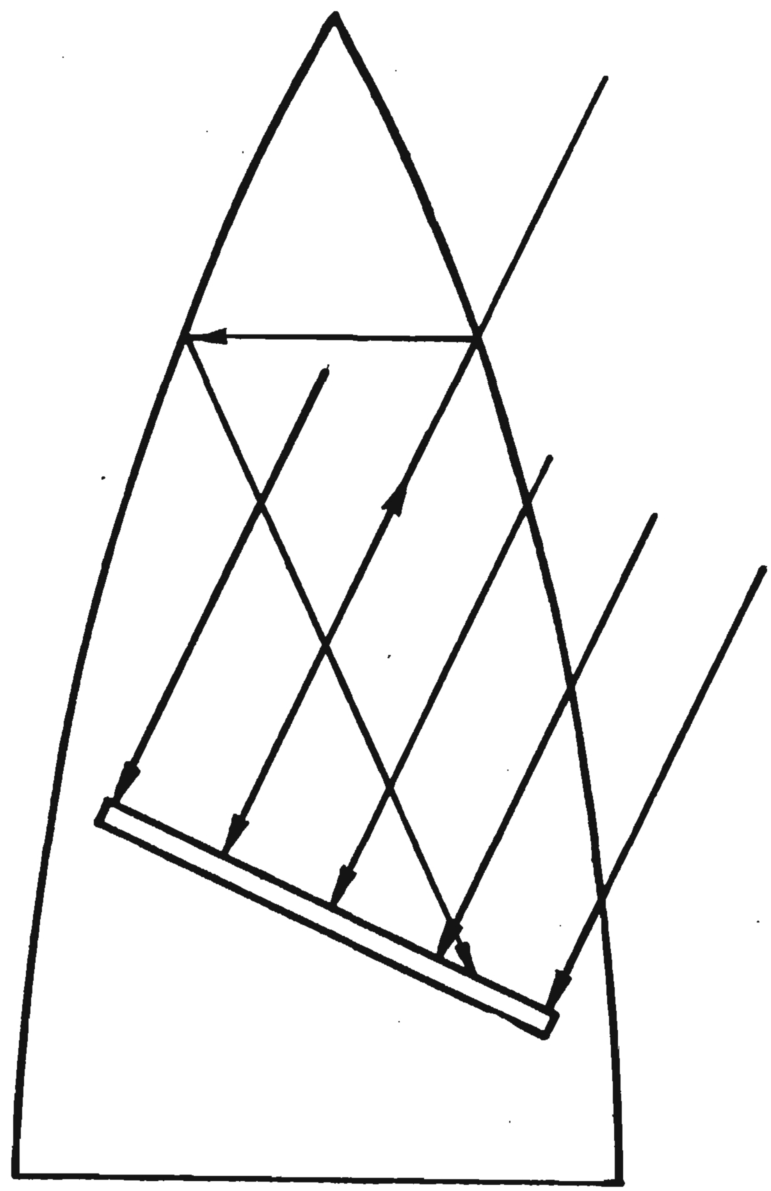

Figure 3-3. Antenna Scattered Energy Added to Backward Ray Trace.

then the ray is discarded. If the ray strikes the radome wall the intersection point is found using numerical techniques and the new direction of the ray and effects of reflection on the ray are calculated as above. The ray is then tested to see if it strikes the antenna. If it does strike the antenna it is summed, if not the ray is dropped.

4.0 COMPARISON OF THEORETICAL AND MEASURED RADOME DATA

4.1 Radome Description

The radome posed for theoretical analysis was a tangent ogive having the basic geometry defined in Figure 4-1; for this geometry the values of the various wall parameters are:

$$D = 13.46 \text{ in.}$$
$$L = 48.47 \text{ in.}$$
$$\Delta = 10.75 \text{ in.}$$
$$\delta = 0 \text{ in.}$$
$$d = 10.7 \text{ in.}$$

In addition, the monolithic wall was specified to have a dielectric constant of 5.0 and loss tangent of 0.005.

The wall thickness specified for the test radome was a sophisticated prescription summarized in Table 4-1. To model this in the program, a closed form expression for radome wall thickness was derived as:

$$\text{THK (inches)} = (0.282 + 0.0064\theta^2) \cdot \text{COS}\left(\frac{(\text{DIST} -34 -4\theta)}{34 - 4\theta}\right)(0.5 + 0.108 \text{ abs } (\theta -0.628) \qquad (4\text{-}1)$$

Where

DIST = Station referenced to radome tip (inches)

θ = Radome circumferential angle from vertical (radians)

The radome roll angle reference, antenna geometry and polarization are depicted in Figure 4-2. The theoretical radome thickness resulting from the use of equation (4-1) is tabulated in Table 4-2.

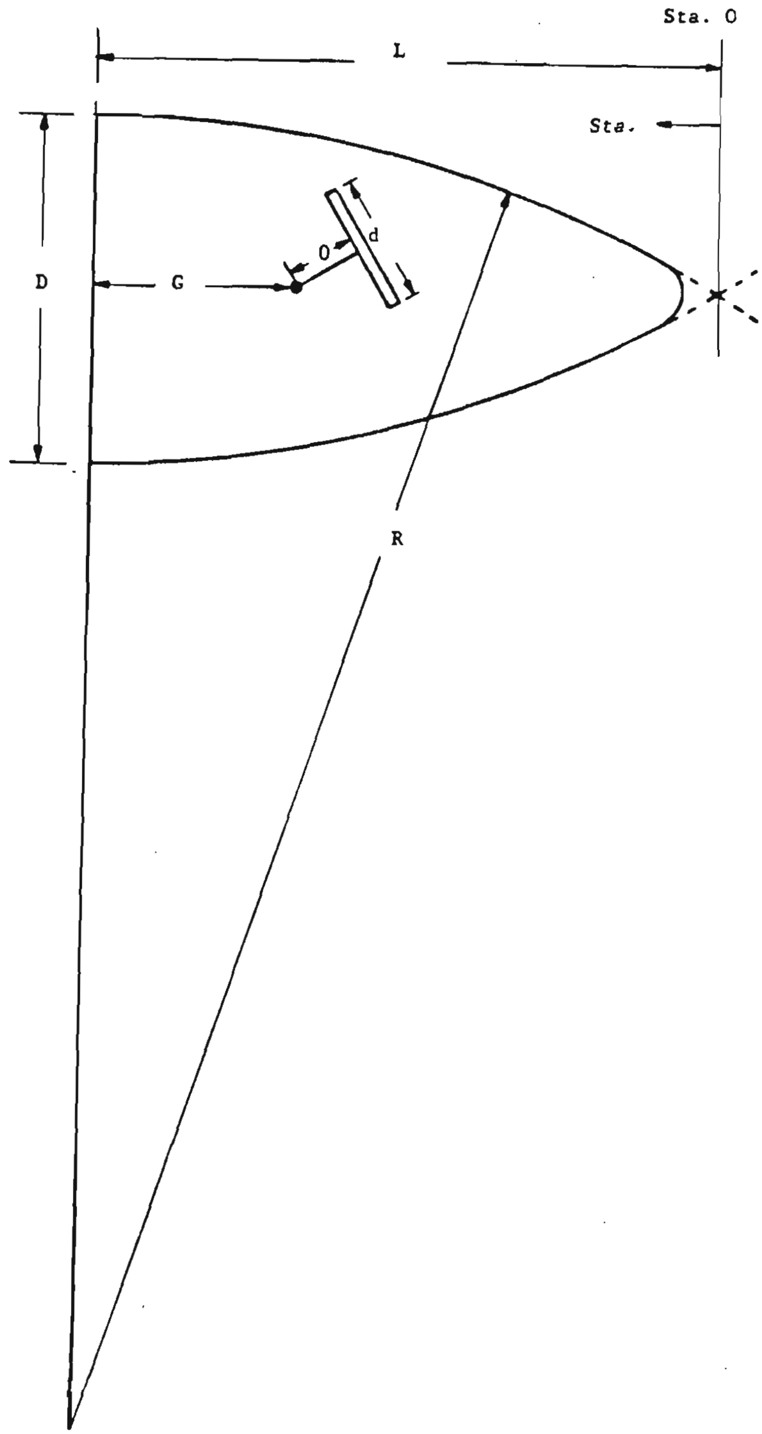

Figure 4-1. Geometry for Tangent Ogive Radome Performance Calculations.

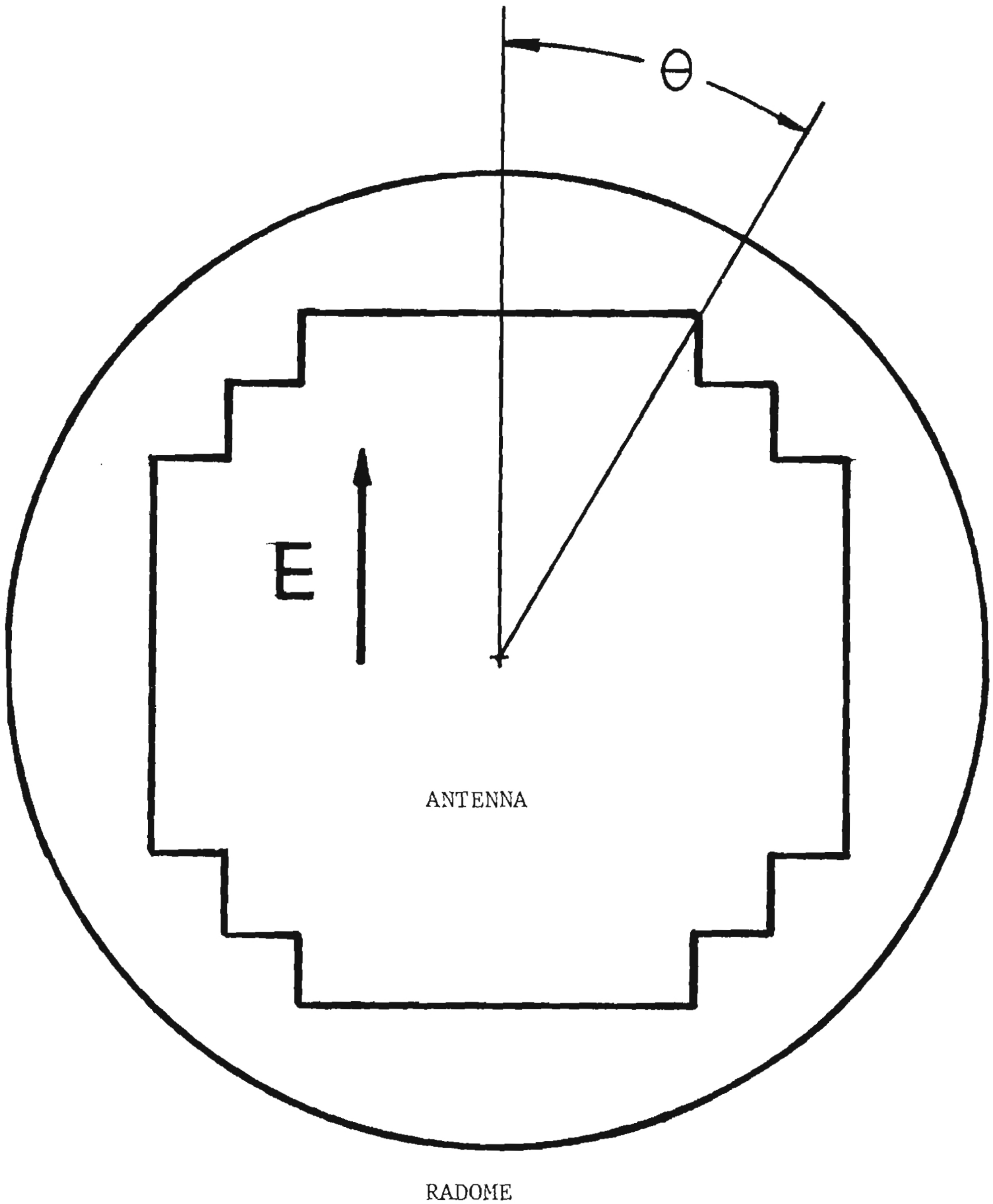

Figure 4-2. Antenna Orientation for Thickness Taper Prescription

TABLE 4-1

WALL THICKNESS VERSUS DISTANCE FROM BASE (DIST)

THETA

DIST	0	22.5	45	67.5	9
0	.238	.246	.250	.249	.248
2	.238	.246	.250	.249	.248
4	.247	.253	.273	.278	.279
6	.251	.259	.276	.281	.284
8	.255	.260	.277	.282	.285
10	.259	.270	.267	.282	.284
12	.258	.267	.259	.285	.287
14	.267	.259	.259	.262	.288
16	.271	.283	.261	.290	.276
18	.273	.273	.270	.291	.280
20	.274	.267	.280	.285	.290
22	.269	.269	.275	.291	.268
24	.265	.281	.263	.274	.274
26	.278	.271	.288	.266	.295
28	.283	.274	.281	.300	.297
30	.285	.281	.275	.281	.297
32	.281	.280	.278	.280	.291
34	.281	.276	.282	.281	.290
36	.281	.282	.279	.283	.283
38	.281	.281	.280	.284	.283
40	.281	.277	.280	.278	.279
42	.275	.275	.279	.276	.275
44	.272	.271	.279	.276	.275
46	.271	.267	.271	.284	.274

THETA (deg)

Distance from Base (in)	0	22.5	45	67.5	90
0	0.2377466481	0.2448168637	0.2485762907	0.2465428489	0.2454710513
2	0.2426787305	0.2492868444	0.253171747	0.2522585635	0.252558735
4	0.2473400924	0.2534950975	0.2574829753	0.2576061945	0.2591702031
6	0.251725534	0.2574372047	0.2615051354	0.2625779389	0.2652929893
8	0.255830163	0.2611090271	0.2652337118	0.2671665422	0.2709155486
10	0.2596494005	0.2645067098	0.2686645185	0.271365309	0.2760272794
12	0.2631789859	0.2676266854	0.2717937039	0.2751681125	0.2806185431
14	0.2664149819	0.2704656782	0.2746177548	0.2785694039	0.2846806827
16	0.2693537785	0.2730207077	0.277133501	0.2815642203	0.2882060387
18	0.2719920973	0.2752890911	0.2793381179	0.2841481917	0.2911879638
20	0.2743269952	0.2772684471	0.2812291306	0.2863175477	0.2936208354
22	0.2763558674	0.2789566974	0.282804416	0.2880691229	0.2955000663
24	0.2780764507	0.2803520695	0.2840622057	0.2894003616	0.2968221129
26	0.2794868257	0.2814530984	0.2850010875	0.2903093211	0.2975844825
28	0.2805854189	0.2822586281	0.2856200074	0.2907946752	0.2977857375
30	0.2813710049	0.282767813	0.2859182706	0.2908557157	0.2974254986
32	0.2818427074	0.2829801183	0.2858955422	0.2904923535	0.2965044449
34	0.282	0.2828953213	0.2855518477	0.2897051188	0.2950243132
36	0.2818427074	0.2825135109	0.284887573	0.2884951604	0.2929878943
38	0.2813710049	0.281835088	0.2839034638	0.2868642437	0.2903990281
40	0.2805854189	0.2808607649	0.282600625	0.2848147485	0.287262596
42	0.2794868257	0.2795915646	0.2809805192	0.2823496653	0.2835845119
44	0.2780764507	0.2780288195	0.2790449653	0.279472591	0.2793717111
46	0.2763558674	0.2761741704	0.2767961362	0.2761877238	0.2746321372

Table 4-2. Theoretical Wall Thickness Model.

4.2 Comparison of Measured and Predicted Data

The boresight errors for the azimuth and elevation principal plane scans are shown in Figures 4-3 and 4-4. Here the same general features are found in both the measured and the calculated curves; for both plus and minus azimuth values the boresight error curve approximates a sine curve for one half of a cycle. The azimuth BSE, curves differ by about 3 milliradians between the calculated and measured while the calculated and measured curves for the elevation scans agree within 2 milliradians over most of the scan.

Similar data, but with added -20 dB rear bulkhead reflections, appear in Figures 4-5 and 4-6. The affects of -15 dB rear bulkhead reflections appear in Figures 4-7 and 4-8.

These bulkhead reflection components noticeably made the computed curves approach the measured curve, especially in the elevation scan. The affects of antenna backwall reflections were then investigated in Figures 4-9 and 4-10. The computed curves come more closely to the measured curves, but the affect due to sidewall reflections in this case was at most .3 milliradians.

The errors including antenna scattered energy were also calculated but not plotted here since the maximum affect of the energy was about 0.1 milliradians.

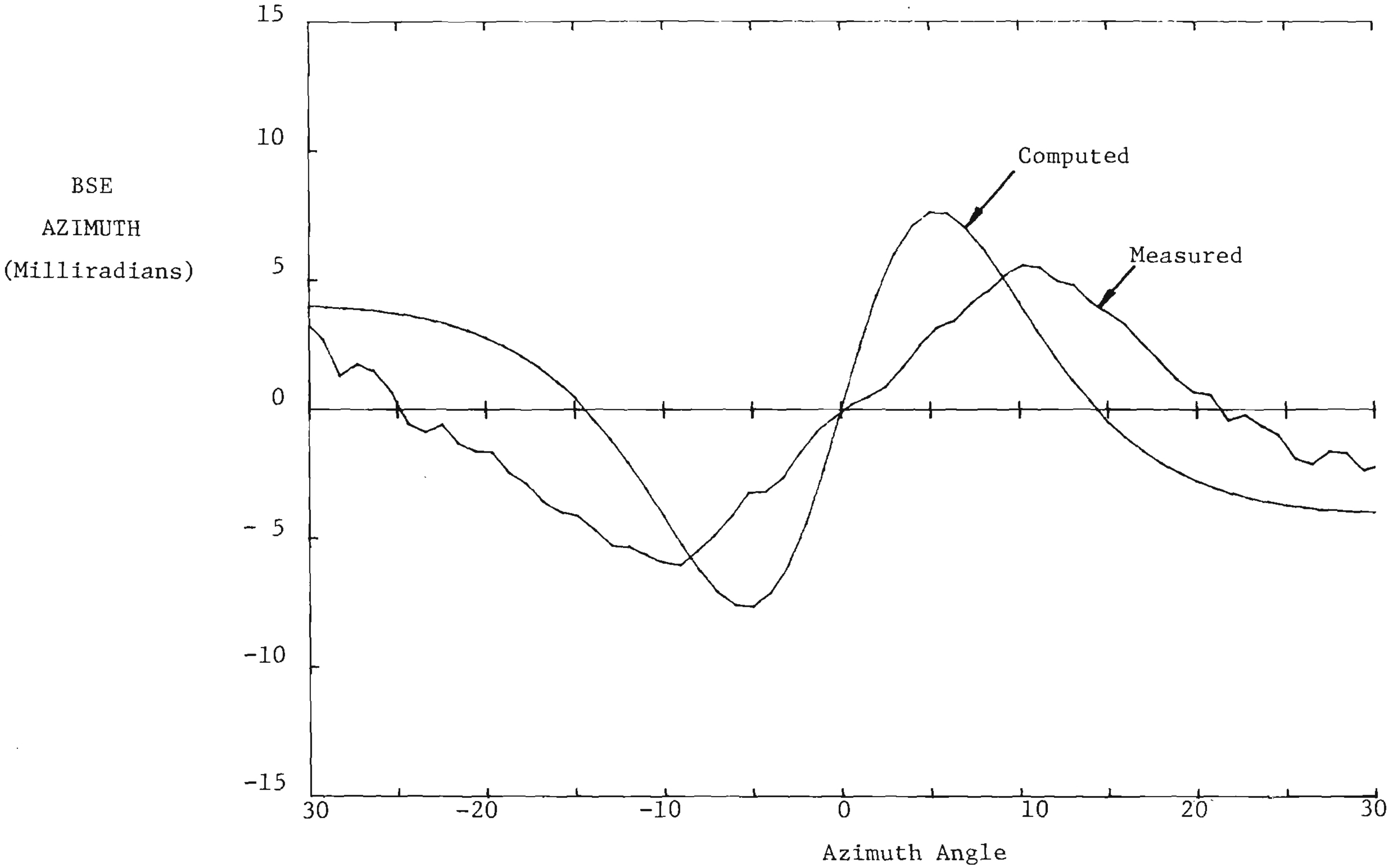

Figure 4-3. Azimuth Scan BSE (no Added Reflections)

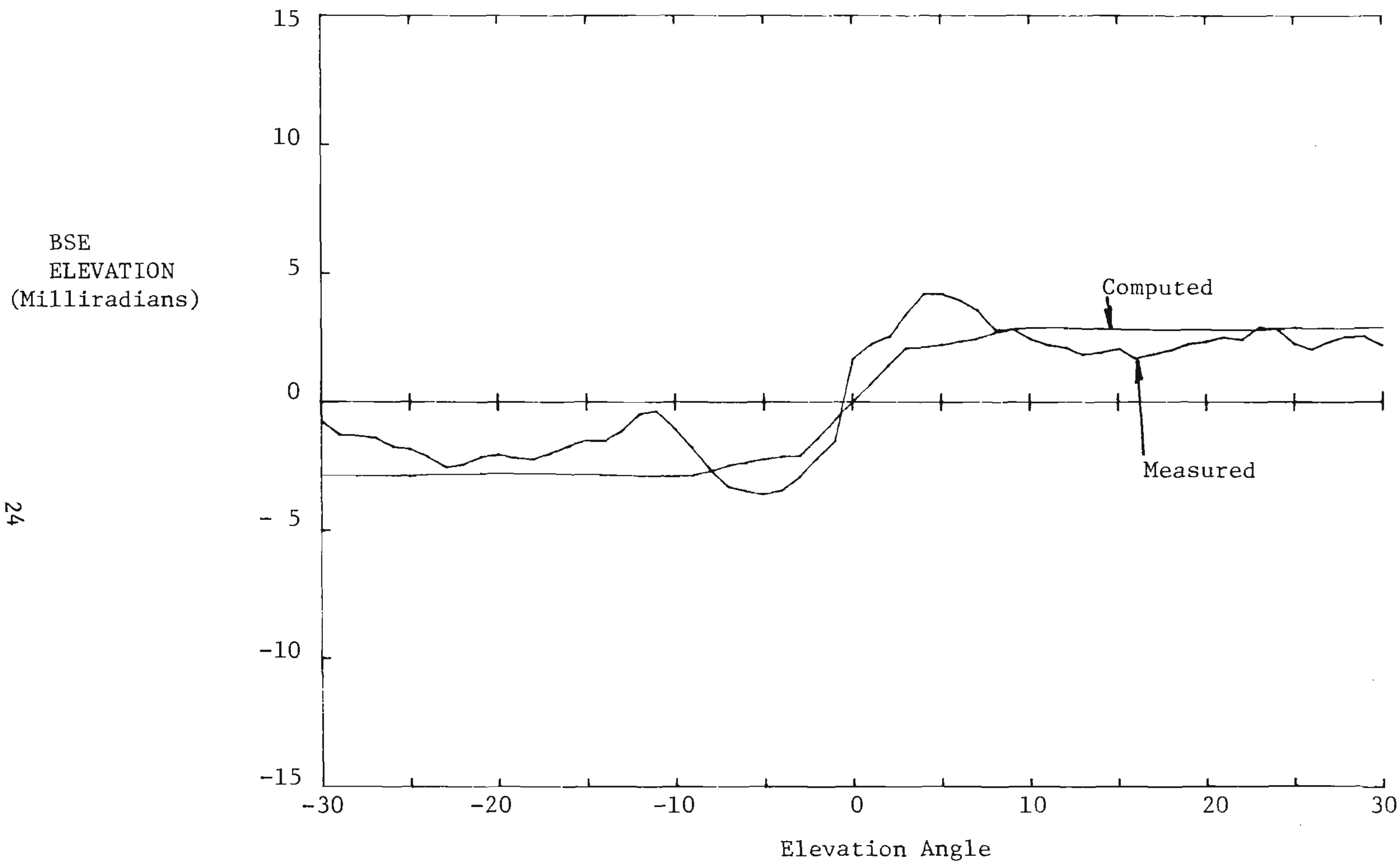

Figure 4-4. Elevation Scan BSE (no Added Reflections)

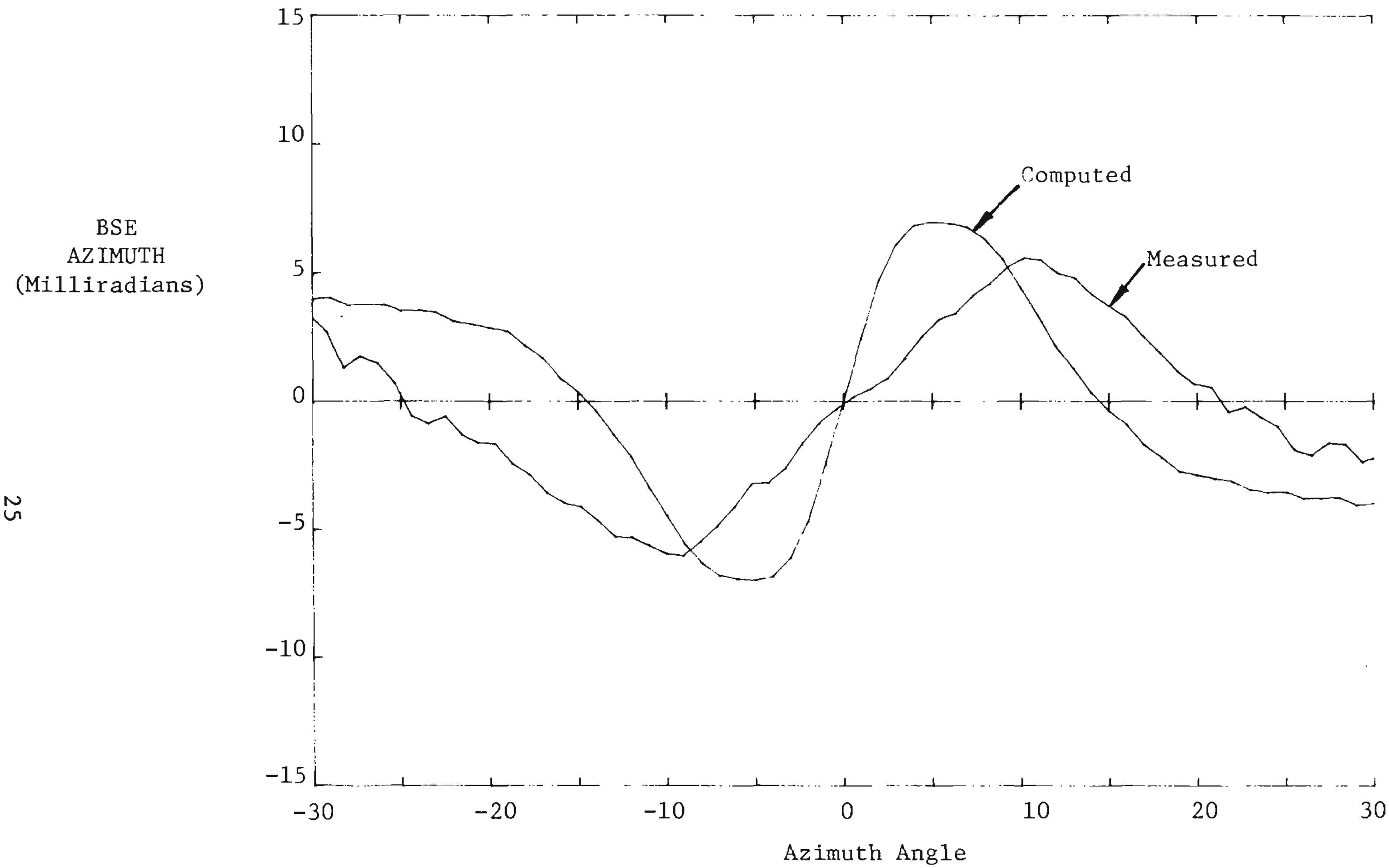

Figure 4-5. Azimuth Scan BSE with Bulkhead Reflection of -20 dB

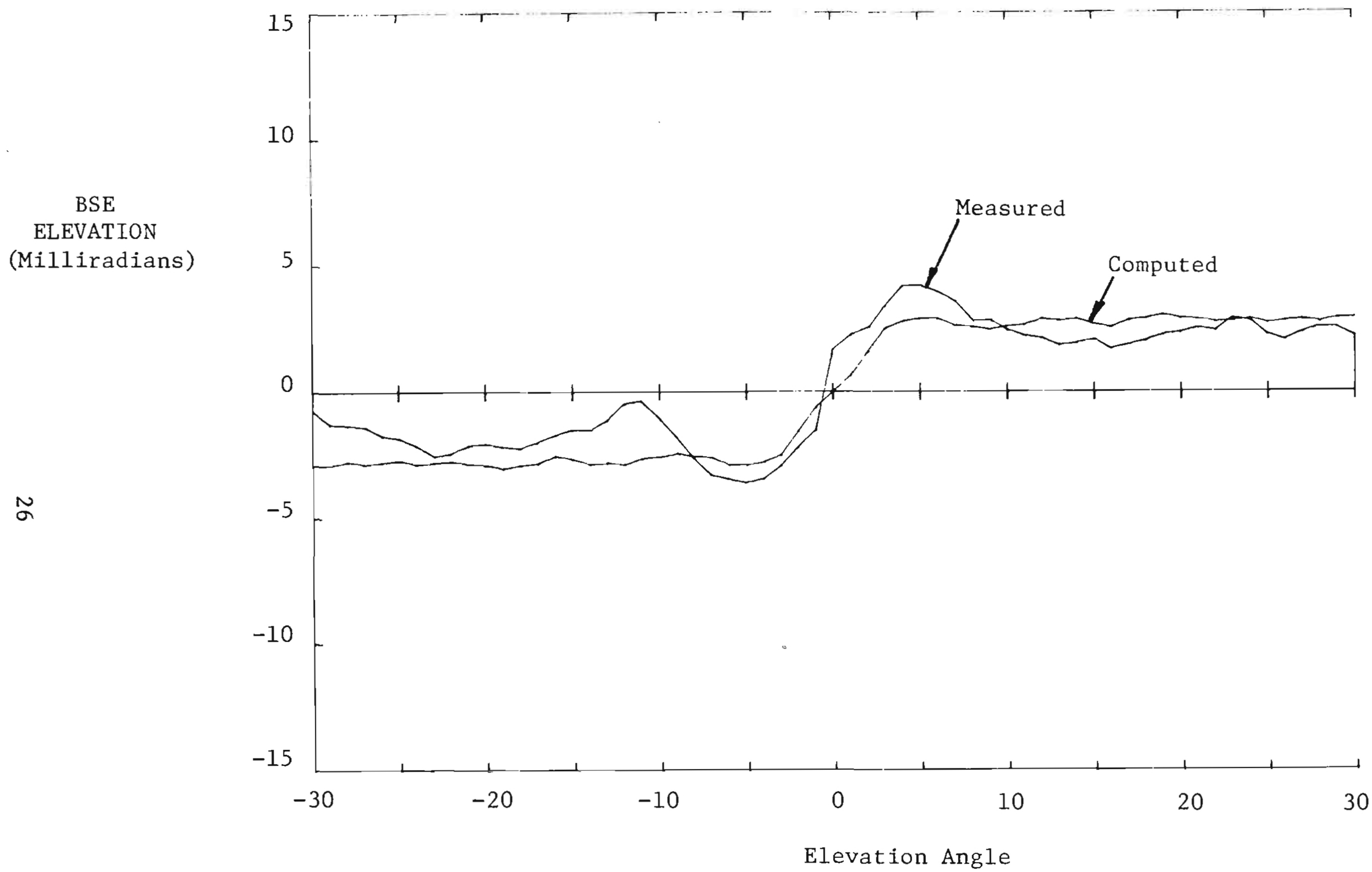

Figure 4-6. Elevation Scan BSE with Bulkhead Reflection of -20 dB

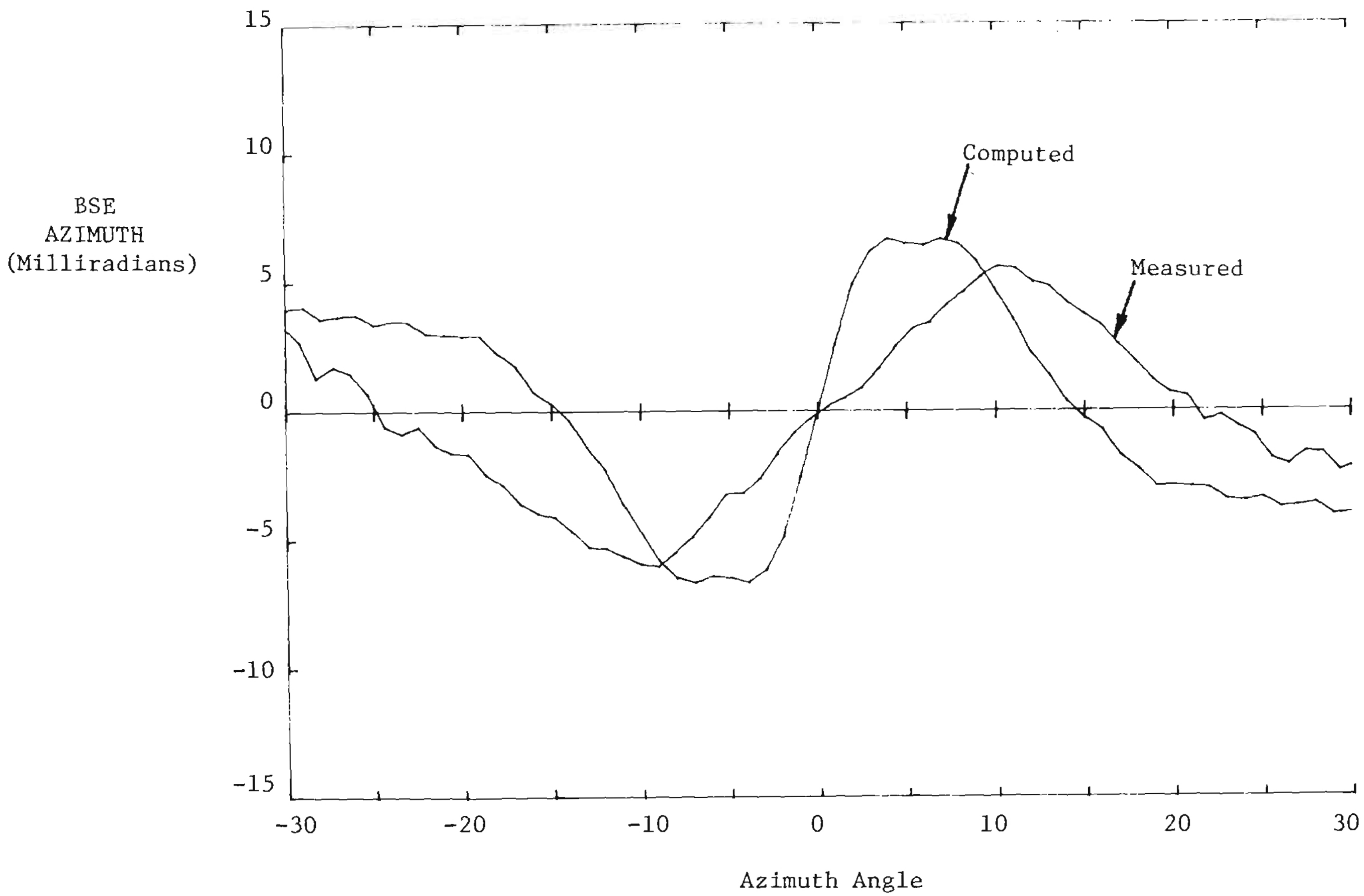

Figure 4-7. Azimuth Scan BSE with Bulkhead Reflection of -15 dB

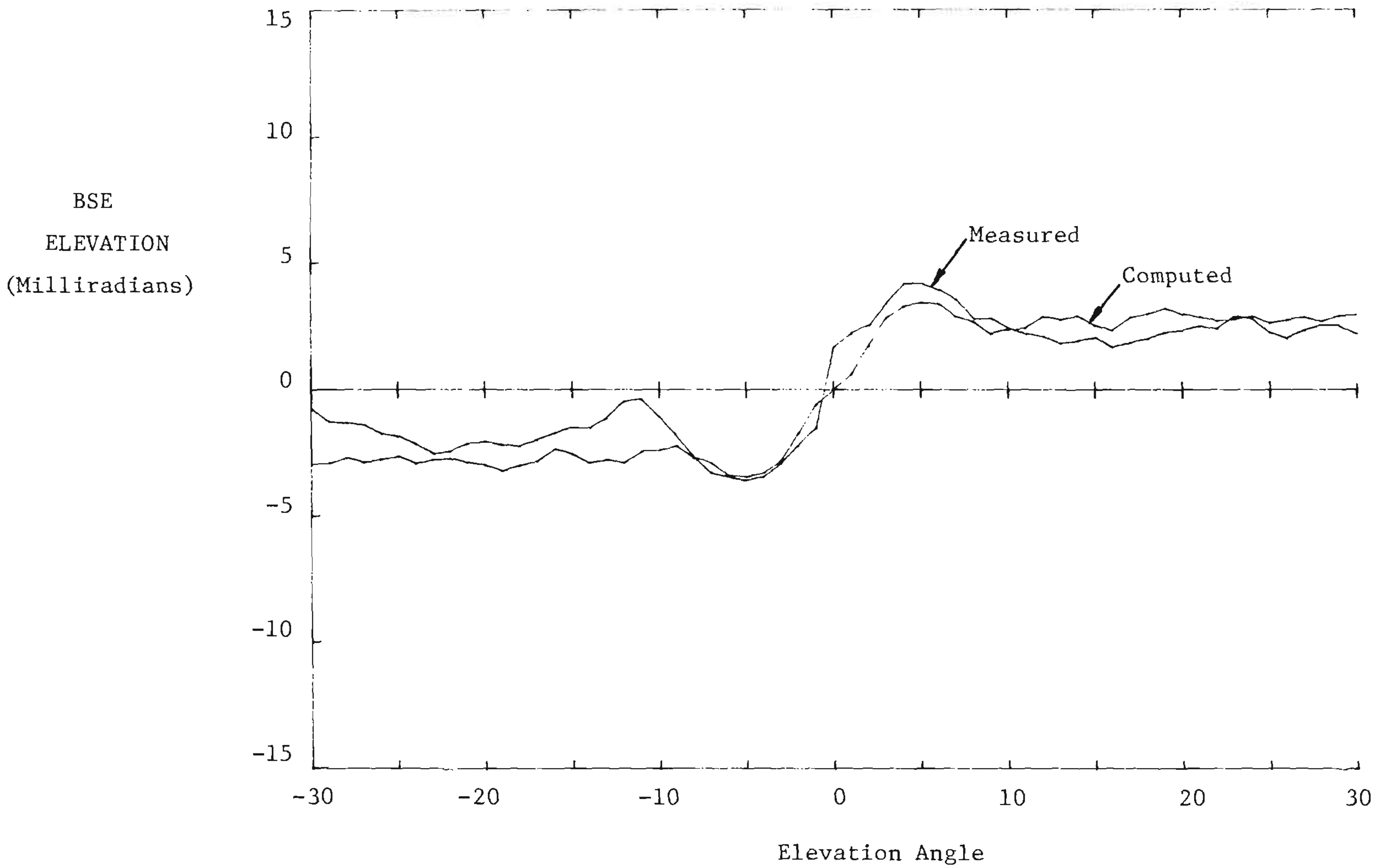

Figure 4-8. Elevation Scan BSE with Bulkhead Reflection of -15 dB

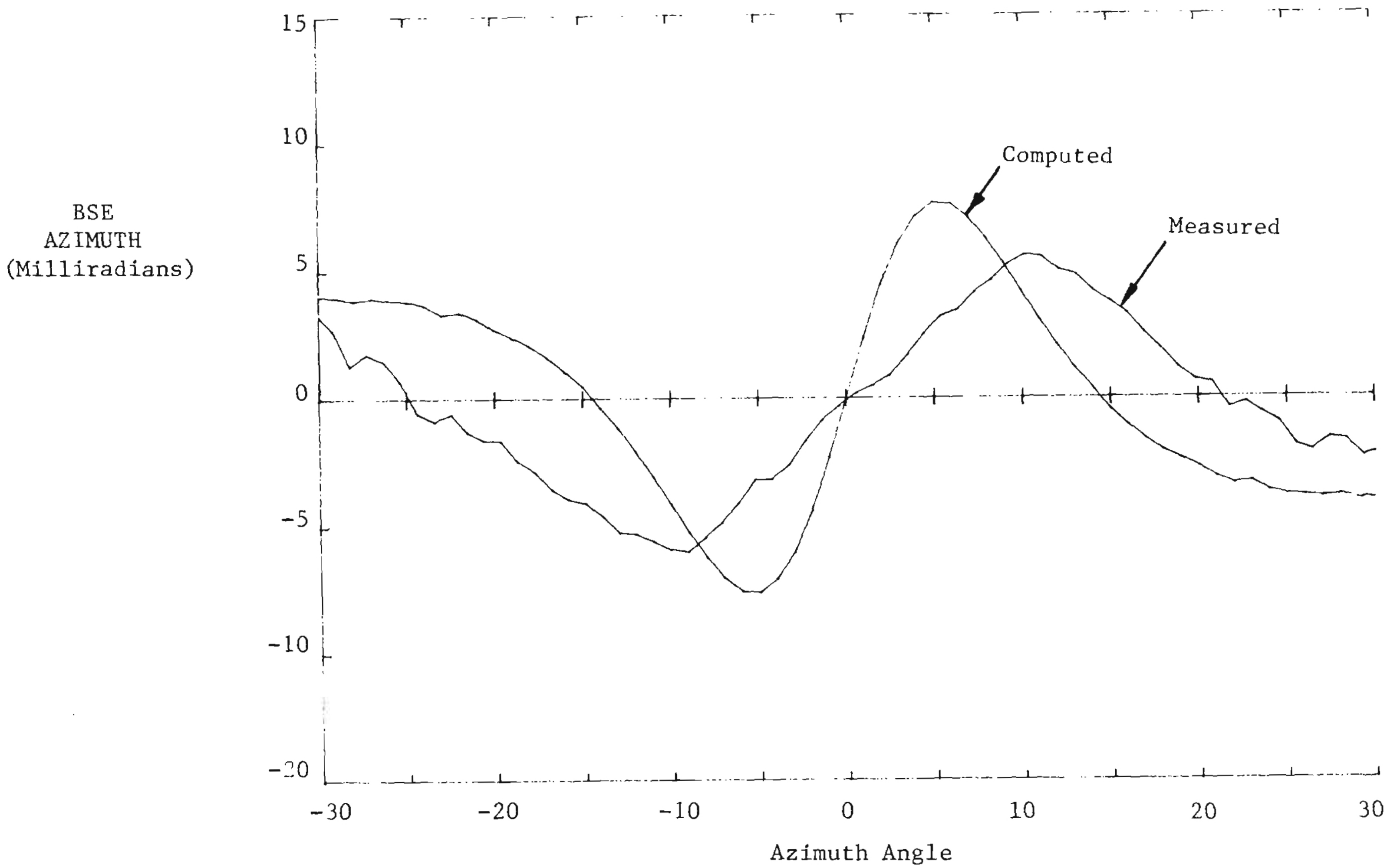

Figure 4-9. Azimuth Scan BSE with Sidewall Reflection Included

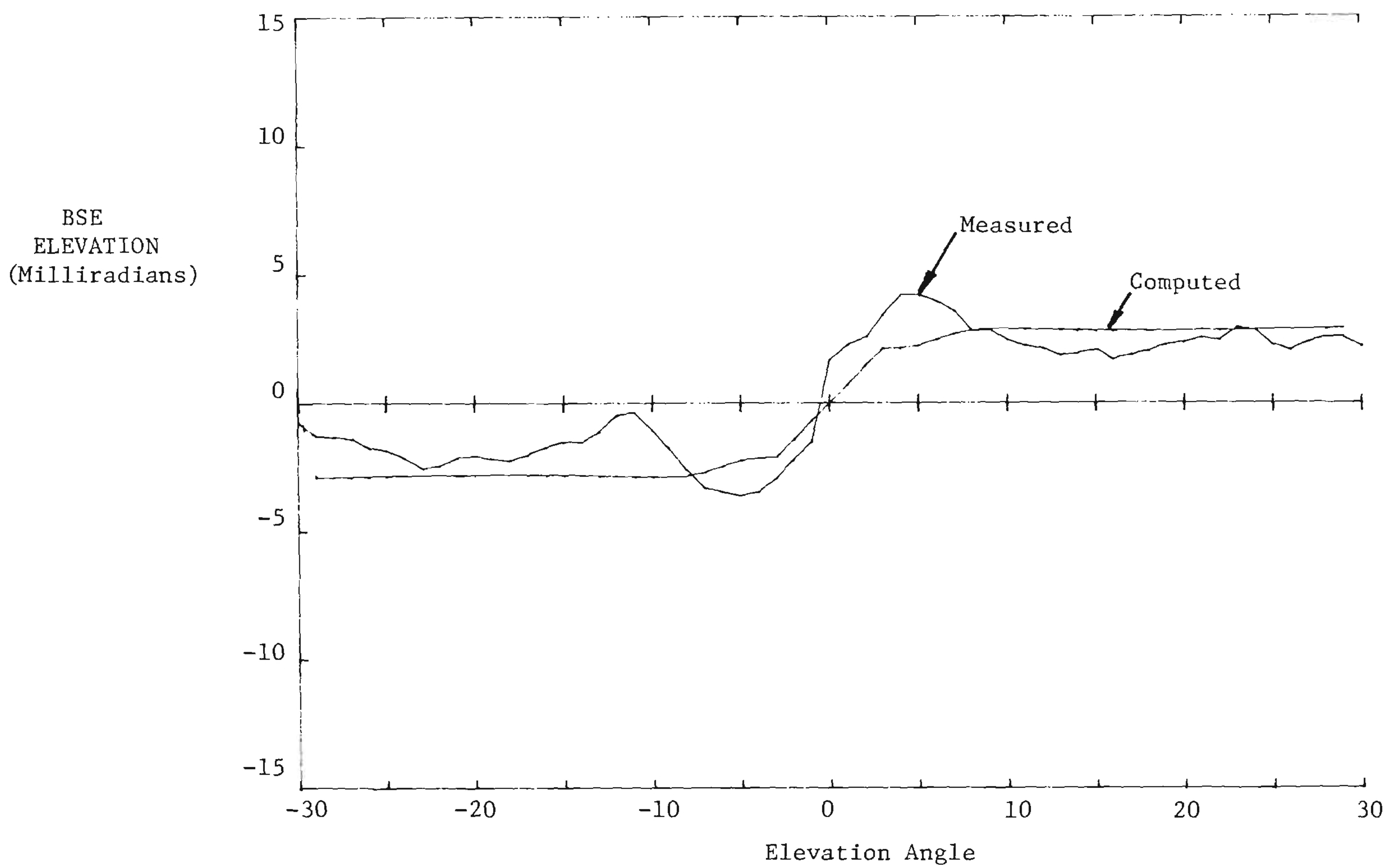

Figure 4-10. Elevation Scan BSE with Sidewall Reflection Included

5.0 Evaluation of Wall Transmission Model

5.1 General

An evaluation of possible sources of computational errors suggested that the wall transmission subroutine used in the computer analysis be considered. Here, the theoretical approach is a matrix solution developed by Collin [1] who formulated expressions based on reflection and transmission components at each boundary of a multilayer dielectric media.

In the domain of geometrical optics, radome walls are approximated as being locally flat and infinite in extent. The method is based on this approximation, and is not valid for thick, highly curved walls. An incident electromagnetic wave is decomposed into components with the electric field vector perpendicular and parallel to the plane of incidence, that plane being defined as containing both the local normal to the surface and the direction vector of propagation. Arbitrary incidence angles, electrical properties, layer thickness, and number of layers can be handled. The method assumes that the dielectric and magnetic properties must be homogeneous and isotropic within individual layers.

A modification can be made for anisotropic materials [4], but added computer time cannot be justified when the anistropy is not large. Multiple reflections between the layer boundaries are analyzed by complex matrix multiplications, one matrix being needed for each boundary. The mathematics for setting up the matrices is based on solving a boundary value problem at each interface.

Applicable Equations

In terms of the layer geometry, and following the development in references [1] and [2], the applicable matrix solution is:

$$\begin{bmatrix} c_1 \\ b_1 \end{bmatrix} = \prod_{i=1}^{N} \left\{ \frac{1}{T_i} \begin{vmatrix} e^{j\Phi_i d_i} & R_i e^{-j\Phi_i d_i} \\ R_i e^{j\Phi_i d_i} & e^{-j\Phi_i d_i} \end{vmatrix} \right\} \cdot \left\{ \frac{1}{T_{N+1}} \begin{vmatrix} 1 & R_{N+1} \\ R_{N+1} & 1 \end{vmatrix} \right\} \begin{bmatrix} c_{N+1} \\ b_{N+1} \end{bmatrix} \tag{1}$$

where N = number of layers,

d_i = i th layer thickness (inches) $T_i = 1 - R_i$, and

$$\Phi_i = k_o\,(\varepsilon_i' - \sin^2\theta)^{1/2} \tag{2}$$

$$R_i = \frac{Z_i - Z_{i-1}}{Z_i + Z_{i-1}} \tag{3}$$

Note: $Z_0 = Z_{N+1} = 1$

$$Z_i = \frac{\cos\theta}{(\varepsilon_i - \sin^2\theta)^{1/2}} \quad \text{(TE or perpendicular polarization)} \tag{4}$$

$$= \frac{(\varepsilon_i - \sin^2\theta)^{1/2}}{\varepsilon_i \cos\theta} \quad \text{(TM or parallel polarization)} \tag{5}$$

Further refinement is made via equation (2) modification:

$$\Phi_i' = k_o\sqrt{\varepsilon_i - \sin^2\theta} \tag{6}$$

$$\Phi_i' = k_o\sqrt{(\varepsilon_i' - \sin^2\theta) - j(\varepsilon_i'')} =$$

$$= k_o\sqrt{\varepsilon_i' - \sin^2\theta}\left\{1 - \frac{j\varepsilon_i' \tan\delta_i}{(\varepsilon_i' - \sin^2\theta)}\right\}^{1/2} \tag{7}$$

$$\Phi_i' \approx k_o\sqrt{\varepsilon_i' - \sin^2\theta}\left\{1 - \frac{j\varepsilon_i' \tan\delta_i}{2(\varepsilon_i' - \sin^2\theta)}\right\} \tag{8}$$

Where in terms of the relative dielectric constant and loss tangent:

$$\varepsilon_i = \varepsilon_i' - j\varepsilon_i'' = \varepsilon_i' (1 - j \tan \delta_i) \tag{9}$$

$$\text{Defining, } \alpha_i = \frac{k_o \varepsilon_i' \tan \delta_i}{2(\varepsilon_i' - \sin^2 \theta)^{1/2}} = \frac{K_o^2 \tan \delta i}{2\Phi_i} \tag{10}$$

Then (7) becomes,

$$\Phi_i' = k_o \sqrt{\varepsilon_i' - \sin^2 \theta} - j\alpha_i$$

$$= \Phi_i - j\alpha_i \tag{11}$$

From which (1) can be expressed:

$$\begin{bmatrix} c_1 \\ \\ b_1 \end{bmatrix} = \frac{1}{T_1 T_2 T_3 T_4 T_5} \prod_{i=1}^{4} \begin{vmatrix} e^{-j\Phi_i' d_i + \alpha_i d_i} & R_i e^{+j\Phi_i' d_i - \alpha_i d_i} \\ \\ R_i e^{-j\Phi_i' d_i + \alpha_i d_i} & e^{+j\Phi_i' d_i - \alpha_i d_i} \end{vmatrix} \tag{12}$$

$$\begin{vmatrix} 1 & R_5 \\ \\ R_5 & 1 \end{vmatrix} \begin{bmatrix} c_6 \\ \\ b_6 \end{bmatrix}$$

or,

$$\begin{bmatrix} c_1 \\ \\ b_1 \end{bmatrix} = \begin{bmatrix} A_{11} & A_{12} \\ \\ A_{21} & A_{22} \end{bmatrix} \begin{bmatrix} c_{N+2} \\ \\ b_{N+2} \end{bmatrix} \tag{13}$$

The voltage transmission coefficient is

$$|T| = 20 \log (c_6/c_1) = -20 \log |A_{11}| \tag{14}$$

The voltage reflection coefficient is

$$|R| = 20 \log (b_1/c_1) = 20 \log |A_{21}/A_{11}| \tag{15}$$

The insertion phase is defined as the difference in electrical thickness between the panel and that of free space over the same thickness as the panel [3].

C_1 is incident on the wall and C_{N+2} is transmitted then

$$C_{INC} = A_{11} C_{TRAN} \tag{16}$$

$$C_{TRAN} = \frac{C_{INC}}{A_{11}} \tag{17}$$

$$\text{angle } (C_{TRAN}) = \text{angle } (C_{INC}) - \text{angle } (A_{11}) \tag{18}$$

$$IPD = -\text{angle } (A_{11}) - \frac{360 \ d(\text{total})}{\lambda} \cos \theta \quad \text{(degrees)} \tag{19}$$

A phase delay also is incurred on the reflecting ray, b_1.

$$B_{refl} = A_{21} C_{TRAN}$$

$$= \frac{A_{21}}{A_{11}} C_{INC} \tag{20}$$

$$\text{angle } (B_{refl}) = \text{angle } (C_{INC}) + \text{Angle } (A_{21}) - \text{Angle } (A_{11}) \tag{21}$$

Limitations

This method computes the transmission coefficient and insertion phase dealy for a plane wave incident at angle θ on a N-layer dielectric sheet with free space on either side; relative permeability of all layers is assumed unity.

There are no restrictions on the range of any of the variables except loss tangent. Here, the approximation made is seen in equation (7). This approximation generally restricts accuracy for loss tangents greater than about 0.10.

5.2 Comparison of Measured and Predicted Data

To assess program accuracy, a sheet of 0.375-inch plexiglass (polymethyl methacrylate) was evaluated The dielectric properties at X-band published in the technical literature indicate a value of $\varepsilon = 2.59$ and $\tan \delta = 0.0067$. These values were input to the wall program to compute the parallel and perpendicular transmission coefficient and insertion phase delay (IPD).

Utilizing the measurements facility at MICOM in conjunction with the Georgia Tech radome measurements instrumentation system, actual data were obtained on a sheet approximately four-feet square. The range of incidence angles measured was limited by the radome positioner to angles less than 60 degrees.

The measured date did not include any reference measurements for the free space or "no sheet" case. The measured transmission was set to 1 and the measured IPD was set to 0 for an incidence angle of 0 degrees. The computed IPD was also set to 0 for 0° incidence angle for comparison with the measured. (These offsets are not important for radome analysis since they effect all rays entering the radome equally.)

The measured and computed values for the transmission and IPD are shown in Figures 5-1 and 5-2. The parallel polarization case had the most difference between measured and computed values for both transmission and IPD coefficients. At 60° the measured IPD differs from the computed by approximately 2 degrees (or 15%) and the measured transmission differs from the computed by approximately -0.05 (or 6%).

The measured data was actually an average of three trials. The IPD and transmission coefficients did vary from trial to trial, but the average would seem to have a low standard deviation as evidenced by the smoothness of the measured curves. The computed curves depend on the thickness and electrical properties of the plexiglass, both of which may have moderate tolerances in the commercial sheet used.

The deviation between measured and computed coefficients is large enough to effect radome boresight errors, particularly for large angles of incident (high fineness ratio radomes). It is the opinion of the authors that some of the descrepancy between measured and computed data is due to measurement errors. While it is difficult to quantify the measurement error component magnitude, it does suggest that if computed radome data is to be compared with actual radome data measured in the same facility, one should factor the measurement data into the data evaluation. Secondly, the measured data herein suggests a theoretical descrepancy of the mathematical model for large angles-of-incidence which can only be resolved via a more exhaustive perfection of the WALL transmission formulation.

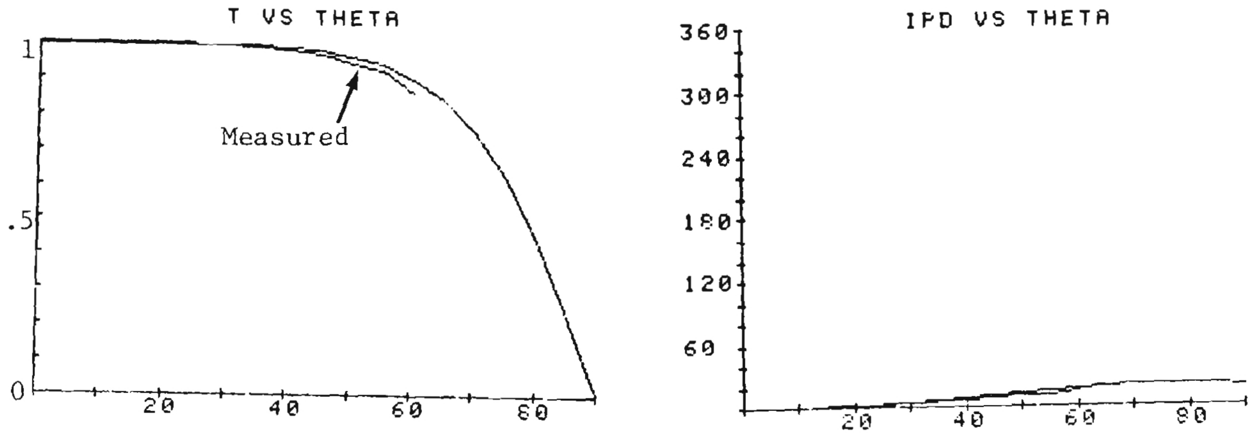

(a) Parallel Polarization

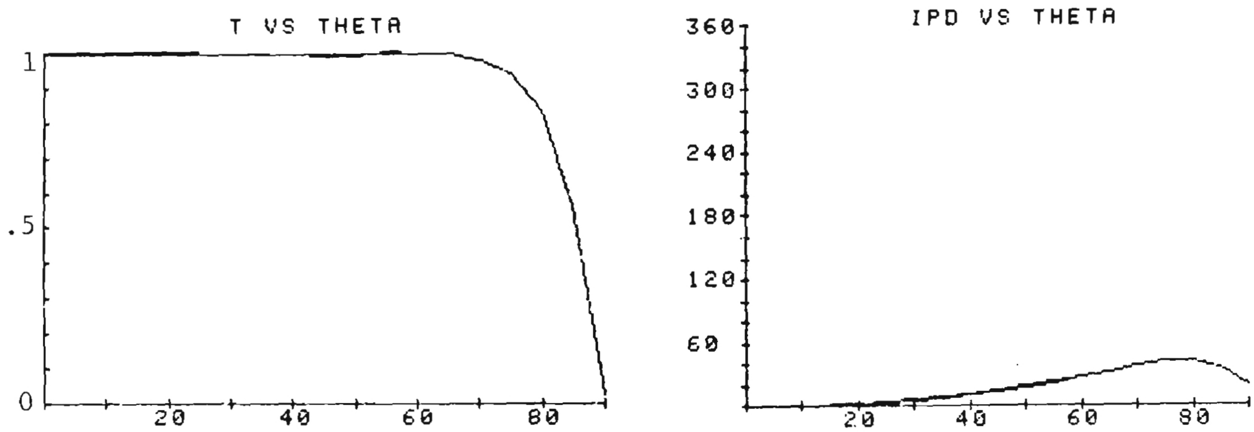

(b) Perpendicular Polarization

Figure 5-1 Comparison of Measured to Calculated Transmission and IPD Values

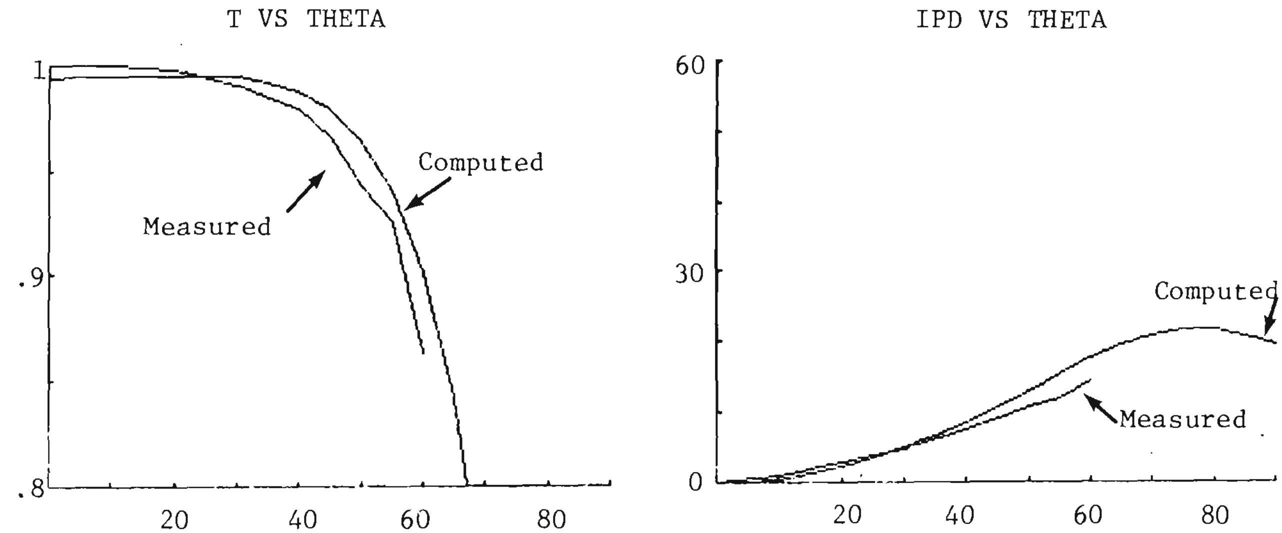

(a) Parallel Polarization

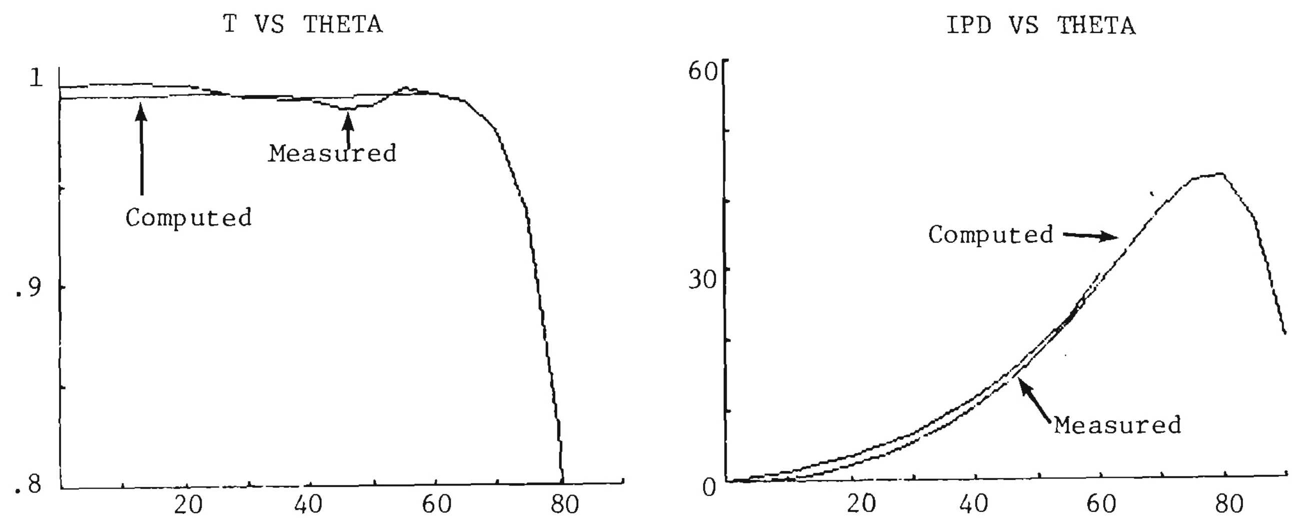

(b) Perpendicular Polarization

Figure 5-2 Close Up of Comparison of Measured to Calculated Transmission and IPD Values

6.0 REFERENCES

1. R. E. Collin, "Field Theory of Guided Waves," McGraw-Hill Book Company, New York, 1960.

2. C. H. Krueger, Jr., "A Computer Program for Determining the Reflection and Transmission Properties of Plane Impedance Boundaries," Report AFATL-TR-67-191, Research and Technology Division, Wright-Patterson AFB, Ohio, September, 1967.

3. H. Jasik, "Antenna Engineering Handbook," McGraw Hill Book Company, New York, 1961.

4. D. J. White and D. J. Banks, "Plane Wave Transmission and Reflection for Anisotropic Sheets of Radome Materials," Proceedings of the Sixteenth Symposium on Electromagnetic Windows, Atlanta, Georgia, June 9-11, 1982.

5. D. J. Kozakoff, G. K. Huddleston and M. West, "Missile Radome Performance Assessment", Final Report on Project A-2939, prepared for U. S. Army Missile Command under Contract DAAH01-81-D-A003, Delivery Order 0015, Georgia Tech, Atlanta, Georgia, December 1981.

APPENDIX A

PROGRAM LISTING

```
      PROGRAM RAD(INPUT,OUTPUT,TAPE5=INPUT,TAPE6=OUTPUT,TAPE7)
      REAL L,LTAN(5),IPD0,IPD1,THK(5),ER(5)
      COMMON/A1/NLAY,ER,LTAN
      COMMON/A2/APAZ,APEL,ILLUM,FREQ,THETA,IPD0,IPD1,RPD0,RPD1
      COMMON/AA2/TRAN0,TRAN1,BKDB,CPHI,SPHI,THK(5)
      COMMON/A3/NRCT1,NARA1,NBLK1,NSAR,VSUM,VDAZ,VDEL
      COMMON/A4/AZS,ELS,AZ,EL,PI,CONV,RSQ,B,THAZ,THEL,EEL,EAZ,L,TIPL
      COMMON/A5/NF,NFIR,D2,ARAD,ADIS,NREF,NARA,NRCT,NANT,NBLK,DBLK
      COMMON/AA5/PY,PZ,DEL
      PI=3.1415927
      CONV=PI/180.
      AZS=0.
      ELS=0.
      NANT=0
      PRINT*,'RAY(1) OR ANTENNA PATTERN(2)'
      READ(5,*)NF
      PRINT*,'ENTER:LENGTH AND DIAMETER OF RADOME(IN.)'
      READ(5,*)L,D
      D2=D/2.
      B=(L*L-D2*D2)/D
      R=B+D2
      RSQ=R*R
      PRINT*,'ENTER ANTENNA DIAMETER'
      READ(5,*)ADIA
      ARAD=ADIA/2.
      PRINT*,'ENTER:APERTURE ILLUMINATION FUNCTION'
      PRINT*,'      1=UNIFORM ILLUMINATION  '
      PRINT*,'      2=COSINE  ILLUMINATION  '
      PRINT*,'      3=TABLE  '
      READ(5,*)ILLUM
      PRINT*,'ANTENNA NPOL.  AZ,EL'
      READ(5,*)APAZ,APEL
      PRINT*,'ENTER:RADOME TIP DIAMETER'
      READ(5,*)TIPD
      TIPL=L-SQRT(RSQ-(B+TIPD/2.)*(B+TIPD/2.))
      PRINT*, 'ENTER # OF PTS PER SIDE (EVEN)'
      READ(5,*)NSAR
      IF(ILLUM.EQ.1) GO TO 78
      PRINT*,'INCLUDE A-R-A REFL. Y(1) N(0)?'
      READ(5,*)NARA
      NARA1=NARA
 78   PRINT*,'INCLUDE WALL REFL. Y(1) N(0)?'
      READ(5,*)NRCT
      NRCT1=NRCT
      PRINT*,'INCLUDE BLKHEAD REFL. Y(1) N(0)?'
      READ(5,*)NBLK
      NBLK1=NBLK
      IF(NBLK.EQ.0) GO TO 80
      PRINT*,'DB'S DOWN FOR BLKHEAD'
      READ(5,*)BKDB
      BKDB=10.**(BKDB/20.)
 80   PRINT*,'DISTANCE TO ANTENNA'
      READ(5,*)DEL
      PRINT*,'EAZ,EEL'
      READ(5,*)EAZ,EEL
      PRINT*,'THAZ,THEL'
      READ(5,*)THAZ,THEL
      THAZ=THAZ*CONV
      THEL=THEL*CONV
```

```
      PRINT*,'ENTER FREQ (GHZ)'
      READ(5,*)FREQ
      NLAY=1
      PRINT*,'ENTER:DIELECTRIC CONST., LOSS TANGENT'
      READ(5,*)ER(1),LTAN(1)
      IF(NF.EQ.2)GO TO 109
      NREF=1
      AZS=1.
      ELS=0.
      CALL ARRAY
      VAZ=VDAZ/VSUM
      AZS=0.
      ELS=1.
      CALL ARRAY
      VEL=VDEL/VSUM
      NREF=0
      ELS=0.
C     EL SCANNER
      AZ=0.
      DO 24 I=1,30
      EL=1.*I
      PRINT*,'EL',EL
      CALL ARRAY
      VT=17.45*(VDEL/VSUM)/VEL
      PRINT*,'BSE',VT
24    CONTINUE
      PRINT*,' '
      EL=0.
      DO 25 I=1,30
      AZ=1.*I
      PRINT*,'AZ',AZ
      CALL ARRAY
      VT=17.45*(VDAZ/VSUM)/VAZ
      PRINT*,'BSE',VT
25    CONTINUE
      STOP
C     ANTENNA PATTERNS
109   PRINT*,'ENTER DIR LOOKED  AZ,EL'
      READ(5,*)AZ,EL
      PRINT*,'ENTER LOWER LIMIT,UPPER LIMIT,INC'
      PRINT*,'FOR AZ SCAN'
      READ(5,*)LLAZ,LUAZ,IAZ
      PRINT*,'FOR EL SCAN'
      READ(5,*)LLEL,LUEL,IEL
      NREF=0
      CALL ARRAY
      RSUM=VSUM
      NANT=1
      I1=LUAZ+IAZ-LLAZ
      I2=LUEL+IEL-LLEL
      DO 106 I=1,I1,IAZ
      AZS=(I-1+LLAZ)*1.
      DO 106 IE=1,I2,IEL
      ELS=(IE-1+LLEL)*1.
      CALL ARRAY
      H3=20.*ALOG10(VSUM/RSUM)
      H1=AZ+AZS
      H2=EL+ELS
106   PRINT*,H1,H2,H3
      STOP
```

```
      END
      SUBROUTINE ARRAY
      COMMON/A2/APAZ,APEL,ILLUM,FREQ,THETA,IPD0,IPD1,RPD0,RPD1
      COMMON/AA2/TRAN0,TRAN1,BKDB,CPHI,SPHI,THK(5)
      COMMON/A3/NRCT1,NARA1,NBLK1,NSAR,VSUM,VDAZ,VDEL
      COMMON/A4/AZS,ELS,AZ,EL,PI,CONV,RSQ,B,THAZ,THEL,EEL,EAZ,L,TIPL
      COMMON/A5/NF,NFIR,D2,ARAD,ADIS,NREF,NARA,NRCT,NANT,NBLK,DBLK
      COMMON/AA5/PY,PZ,DEL
      COMMON/A6/VRSUM,VISUM,VRDEL,VIDEL,VRDAZ,VIDAZ,BKPS
      COMMON/C1/POS(3),K(3),CAN,SAN,RM,PSN(3),S,C(3),NSKP
      COMMON/C2/CAZ,SAZ,CEL,SEL
      COMMON/AR/RAZ,IAZ,REL,IEL,E91,P91,E92,P92,N(3),P7
      COMMON/F1/T,COSF
      REAL IAZ,IEL,I1,I2,N(3),K,L
      NRCT=0
      VRSUM=0.
      VISUM=0.
      VRDEL=0.
      VIDEL=0.
      VRDAZ=0.
      VIDAZ=0.
      NFIR=1
      DO 26 N1=1,NSAR
      DO 26 N2=1,NSAR
      NARA=0
      NBLK=0
      NSKP=0
      PY=(ARAD/NSAR)*(2*N2-NSAR-1)
      PZ=(ARAD/NSAR)*(2*N1-NSAR-1)
      ADIS=SQRT(PY*PY+PZ*PZ)
      IF(ADIS.GT.ARAD) GO TO 26
      CALL RAY
      IF(NREF.EQ.1) GO TO 26
      IF(POS(2)**2+POS(3)**2.LT.D2*D2*.01) GO TO 107
      IF(NARA1.EQ.0) GO TO 107
      NARA=NARA1
      PY1=PY
      PZ1=PZ
      E91=E91*(1.-TRAN0)*(1.-COSF)
      P91=P91+RPD0
      E92=E92*(1.-TRAN1)*(1.-COSF)
      P92=P92+RPD1
      R1=COS(P91)*E91
      I1=SIN(P91)*E91
      R2=COS(P92)*E92
      I2=SIN(P92)*E92
      RAZ=CPHI*R1+SPHI*R2
      IAZ=CPHI*I1+SPHI*I2
      REL=CPHI*R2-SPHI*R1
      IEL=CPHI*I2-SPHI*I1
      P7=T*.531976*FREQ
      CALL BNC(K,N)
      T=-POS(1)/C(1)
      T=(POS(2)+T*C(2))**2+(POS(3)+T*C(3))**2
      IF(T.LT.D2*D2) GO TO 107
      CALL MRF(.01*D2,2.*D2,C)
      P7=P7+T*.531976*FREQ
      Z11=K(1)
      Z12=K(2)
      Z13=K(3)
```

```
      K(1)=C(1)
      K(2)=C(2)
      K(3)=C(3)
      CALL RAY
      K(1)=Z11
      K(2)=Z12
      K(3)=Z13
      PY=PY1
      PZ=PZ1
      NARA=0
107   NBLK=NBLK1
      IF(NBLK.EQ.0.OR.K(1).EQ.1.) GO TO 26
      POS(1)=-CAZ*SEL*PY+SAZ*PZ+DEL
      POS(2)=CEL*PY
      POS(3)=SEL*SAZ*PY+CAZ*PZ
      S1=POS(1)/K(1)
      POS(1)=0.
      POS(2)=POS(2)+S1*K(2)
      POS(3)=POS(3)+S1*K(3)
      IF(SQRT(POS(2)*POS(2)+POS(3)*POS(3)).GT.D2) GO TO 26
      C(1)=K(1)
      C(2)=K(2)
      C(3)=K(3)
      NSKP=2
      CALL RAY
      DBLK=SQRT((PSN(1)-DEL)*(PSN(1)-DEL)+PSN(2)*PSN(2)+PSN(3)*PSN(3))
      IF(DBLK.LT.ARAD)GO TO 26
      BKPS=(S1+S)*FREQ*.531976
      NSKP=0
      CALL RAY
26    CONTINUE
      NSKP=0
      NBLK=0
      NRCT=NRCT1
      IF(NRCT.EQ.0.OR.NREF.EQ.1) GO TO 40
      RM=K(1)/SQRT(K(3)*K(3)+K(2)*K(2))
      TEMP=(L-DEL)/D2
      IF(RM.GT.TEMP) GO TO 40
      RADM=(L-DEL)/RM
      ANG=SIGN(PI/2.,-K(2))
      IF(K(3).NE.0.) ANG=ATAN2(-K(2),-K(3))
      NY=INT(D2*NSAR/(2.*ARAD)+.25)*2
      NZ=INT(RADM*NSAR/(4.*ARAD)+.25)*2
      IF(NZ.EQ.0) GO TO 40
      IF(NY.LT.2) NY=2
      IF(NZ.LT.2) NZ=2
      DO 30 N1=1,NY
      DO 30 N2=1,NZ
      NRCT=1
      PY=(2*N1-NY-1)*D2/NY
      PZ=(2*N2-1)*RADM/(2.*NZ)
      ADIS=SQRT(PY*PY+PZ*PZ)
      IF(ADIS.LT.D2) GO TO 30
      DIS=(RADM-PZ)*RM
      IF(ABS(PY).GT.SQRT(RSQ-(L-DIS)*(L-DIS))-B) GO TO 30
      CAN=COS(ANG)
      SAN=SIN(ANG)
      POS(1)=DEL
      POS(3)=CAN*PZ-SAN*PY
      POS(2)=SAN*PZ+CAN*PY
```

```
      CALL RAY
   30 CONTINUE
   40 CONTINUE
C      BSE FINDER
      VSUM=SQRT(VRSUM*VRSUM+VISUM*VISUM)
      IF(NF.EQ.2) RETURN
      IF(NREF.EQ.1) GO TO 27
      ANSUM=ATAN2(VISUM,VRSUM)
      ANDAZ=ATAN2(VIDAZ,VRDAZ)
      ANDEL=ATAN2(VIDEL,VRDEL)
   27 VDAZ=SQRT(VRDAZ*VRDAZ+VIDAZ*VIDAZ)*SIGN(1.,SIN(ANDAZ-ANSUM))
      VDEL=SQRT(VRDEL*VRDEL+VIDEL*VIDEL)*SIGN(1.,SIN(ANDEL-ANSUM))
      RETURN
      END
      SUBROUTINE RAY
      REAL K(3),N(3),T2(3),IAZ,IEL,I1,I2,I3,IPD0,IPD1,L,PINT(3)
      COMMON/A2/APAZ,APEL,ILLUM,FREQ,THETA,IPD0,IPD1,RPD0,RPD1
      COMMON/A4/AZS,ELS,AZ,EL,PI,CONV,RSQ,B,THAZ,THEL,EEL,EAZ,L,TIPL
      COMMON/AA2/TRAN0,TRAN1,BKDB,CPHI,SPHI,THK(5)
      COMMON/A5/NF,NFIR,D2,ARAD,ADIS,NREF,NARA,NRCT,NANT,NBLK,DBLK
      COMMON/AA5/PY,PZ,DEL
      COMMON/A6/VRSUM,VISUM,VRDEL,VIDEL,VRDAZ,VIDAZ,BKPS
      COMMON/B1/NLST,AR(4),AI(4),BR(4),BI(4),CR(4),CI(4)
      COMMON/C1/POS(3),K(3),CAN,SAN,RM,PSN(3),S,C(3),NSKP
      COMMON/C2/CAZ,SAZ,CEL,SEL
      COMMON/AR/RAZ,IAZ,REL,IEL,E91,P91,E92,P92,N(3),P7
      COMMON/F1/T,COSF
      IF(NARA.EQ.0)  P7=0.
      IF(NSKP.EQ.2) GO TO 990
      IF(NARA.EQ.1) GO TO 63
      IF(NBLK.EQ.1) P7=P7+BKPS
      IF(NRCT.EQ.1.OR.NBLK.EQ.1) GO TO 59
      IF(NF.NE.2.AND.NREF.EQ.0) GO TO 18
      CAZS=COS(AZS*CONV)
      SAZS=SIN(AZS*CONV)
      CELS=COS(ELS*CONV)
      SELS=SIN(ELS*CONV)
      PSH1=SAZS*PZ-CAZS*SELS*PY
      PSH2=CELS*PY
      PSH3=SELS*SAZ*PY+CAZS*PZ
      ALP=ACOS((ABS(PSH2*PY+PSH3*PZ)/(ADIS*ADIS)-1E-8))
      P7=SIGN(SIN(ALP)*ADIS*FREQ*.531976,PSH1)
   18 IF(NREF.EQ.1) GO TO 1000
      IF(NFIR.EQ.0) GO TO 19
      NFIR=0
      H=(AZ+AZS)*CONV
      CAZ=COS(H)
      SAZ=SIN(H)
      H1=(EL+ELS)*CONV
      CEL=COS(H1)
      SEL=SIN(H1)
      IF(NANT.EQ.1) GO TO 19
      K(1)=CAZ*CEL
      K(2)=SEL
      K(3)=-SAZ*CEL
   19 POS(1)=-CAZ*SEL*PY+SAZ*PZ+DEL
      POS(2)=CEL*PY
      POS(3)=SEL*SAZ*PY+CAZ*PZ
C      MOD REGULA FALSI
   59 IF(NRCT.EQ.1) GO TO 62
```

```
      CALL MRF(0.,L+ARAD,K)
      GO TO 63
62    CDIS=SQRT(PZ*PZ+RM*RM*PZ*PZ)
      CALL MRF(CDIS,2.*CDIS,K)
63    POS(1)=POS(1)+T*K(1)
      IF(POS(1).GT.L-TIPL) RETURN
      POS(2)=POS(2)+T*K(2)
      POS(3)=POS(3)+T*K(3)
      N(1)=POS(1)/SQRT(RSQ-POS(1)*POS(1))
      U=SQRT(1+N(1)*N(1))
      N(1)=N(1)/U
      U=U*SQRT(POS(2)*POS(2)+POS(3)*POS(3))
      N(2)=POS(2)/U
      N(3)=POS(3)/U
      T2(1)=K(2)*N(3)-K(3)*N(2)
      T2(2)=K(3)*N(1)-K(1)*N(3)
      T2(3)=K(1)*N(2)-K(2)*N(1)
      U=SQRT(T2(1)*T2(1)+T2(2)*T2(2)+T2(3)*T2(3))
      T2(1)=T2(1)/U
      T2(2)=T2(2)/U
      T2(3)=T2(3)/U
      THETA=ASIN(ABS(U))
      PHI=SIGN(ACOS(T2(1)*SAZ+T2(3)*CAZ),T2(2))
      CPHI=COS(PHI)
      SPHI=SIN(PHI)
      IF(NRCT.EQ.2.OR.NARA.EQ.1) GO TO 23
      RAZ=COS(THAZ)*EAZ
      IAZ=SIN(THAZ)*EAZ
      REL=COS(THEL)*EEL
      IEL=SIN(THEL)*EEL
23    R3=CPHI*RAZ+SPHI*REL
      I3=CPHI*IAZ+SPHI*IEL
      E91=SQRT(R3*R3+I3*I3)
      P91=ATAN2(I3,R3)
      R3=CPHI*REL-SPHI*RAZ
      I3=CPHI*IEL-SPHI*IAZ
      E92=SQRT(R3*R3+I3*I3)
      P92=ATAN2(I3,R3)
C      ADD EFFECTS OF RADOME
      IF(NRCT.NE.2.AND.NARA.NE.1) GO TO 999
      CALL THIC(POS,THK)
      CALL WALL
      E91=E91*(1.-TRANO)/K(1)
      P91=P91+RPDO
      E92=E92*(1.-TRAN1)/K(1)
      P92=P92+RPD1
      CALL BNC(K,N)
990   YM=SEL/(CEL*CAZ)
      ZM=SAZ/CAZ
      S=DEL+POS(3)*ZM-POS(2)*YM-POS(1)
      S=S/(C(1)+C(2)*YM-C(3)*ZM)
      PSN(1)=POS(1)+S*C(1)
      PSN(2)=POS(2)+S*C(2)
      PSN(3)=POS(3)+S*C(3)
      IF(NSKP.EQ.2) RETURN
      IF(NARA.EQ.1) GO TO 996
      D1=PINT(1)-POS(1)
      D4=PINT(2)-POS(2)
      D3=PINT(3)-POS(3)
      PHA=SQRT(D1*D1+D4*D4+D3*D3)+S
```

```
  996 PY=SEL*SAZ*PSN(3)+CEL*PSN(2)-SEL*CAZ*(PSN(1)-DEL)
      PZ=SAZ*(PSN(1)-DEL)+CAZ*PSN(3)
      ADIS=SQRT(PY*PY+PZ*PZ)
      IF(ADIS.GT.ARAD) RETURN
      IF(NARA.EQ.1) GO TO 997
      DIS=ABS((PINT(1)-PSN(1))*K(1)+(PINT(2)-PSN(2))*K(2)
     $+(PINT(3)-PSN(3))*K(3))
      PHA=(PHA-DIS)*.531976*FREQ
      P7=P7+PHA
      GO TO 998
  997 P7=P7+S
      GO TO 998
  999 CALL THIC(POS,THK)
      CALL WALL
      E91=E91*TRANO
      P91=P91+IPDO
      E92=E92*TRAN1
      P92=P92+IPD1
  998 SPHI=-SPHI
      R1=COS(P91+P7)*E91
      I1=SIN(P91+P7)*E91
      R2=COS(P92+P7)*E92
      I2=SIN(P92+P7)*E92
      IF(NRCT.NE.1) GO TO 1000
      RAZ=CPHI*R1+SPHI*R2
      IAZ=CPHI*I1+SPHI*I2
      REL=CPHI*R2-SPHI*R1
      IEL=CPHI*I2-SPHI*I1
      NRCT=2
      PINT(1)=POS(1)
      PINT(2)=POS(2)
      PINT(3)=POS(3)
      POS(1)=DEL
      POS(2)=SAN*PZ+CAN*PY
      POS(3)=CAN*PZ-SAN*PY
      CALL MRF(0.,CDIS,K)
      GO TO 63
 1000 COSF=1.
      IF(NBLK.EQ.1) COSF=COSF*BKDB
      SINFEL=SIGN(1.,PY)
      SINFAZ=SIGN(1.,PZ)
      IF(ILLUM.NE.2) GO TO 50
      COSF=COS(1.24507*ADIS/ARAD)*COSF
      SINFAZ=SIN(PI*PZ/ARAD)
      SINFEL=SIN(PI*PY/ARAD)
   50 AAZ=1.
      AEL=1.
      IF(NRCT.EQ.0.AND.NARA.EQ.0) GO TO 51
      ZM=SQRT(C(1)*C(1)+C(3)*C(3))*SQRT(1-K(2)*K(2))
      YM=SQRT(C(1)*C(1)+C(2)*C(2))*SQRT(1-K(3)*K(3))
      AAZ=(C(1)*K(1)+C(3)*K(3))/ZM
      AEL=(C(1)*K(1)+C(2)*K(2))/YM
   51 IF(NBLK.EQ.0) GO TO 55
      AAZ=COS(2.*ACOS(K(1)/SQRT(1.-K(2)*K(2))))
      AEL=COS(2.*ACOS(K(1)/SQRT(1.-K(3)*K(3))))
   55 IF(NF.NE.2) GO TO 56
      AAZ=AAZ*CAZS*CAZS*CELS*CELS/SQRT(1.-SELS*SELS)
      AEL=AEL*CAZS*CAZS*CELS*CELS/SQRT(1.-SAZS*SAZS*CELS*CELS)
   56 APAZ1=APAZ*AAZ
      APEL1=APEL*AEL
```

```
      IF(NREF.EQ.0) GO TO 52
      RSS=(EAZ*COS(THAZ+P7)*APAZ1+EEL*COS(THEL+P7)*APEL1)*COSF
      ESS=(EAZ*SIN(THAZ+P7)*APAZ1+EEL*SIN(THEL+P7)*APEL1)*COSF
      GO TO 54
52    RSS=((CPHI*R1+SPHI*R2)*APAZ1+(CPHI*R2-SPHI*R1)*APEL1)*COSF
      ESS=((CPHI*I1+SPHI*I2)*APAZ1+(CPHI*I2-SPHI*I1)*APEL1)*COSF
54    VRSUM=VRSUM+RSS
      VISUM=VISUM+ESS
      VRDEL=VRDEL+RSS*SINFEL
      VIDEL=VIDEL+ESS*SINFEL
      VRDAZ=VRDAZ+RSS*SINFAZ
      VIDAZ=VIDAZ+ESS*SINFAZ
      RETURN
      END
      SUBROUTINE MRF(A,B1,K2)
      REAL K1(3),K2(3)
      COMMON/F1/T,COSF
      COMMON/F2/K1
      K1(3)=K2(3)
      K1(2)=K2(2)
      K1(1)=K2(1)
      F=FH(A)
      G=FH(B1)
      W=A
      F2=F
      DO 20 N3=1,5
      W1=(G*A-F*B1)/(G-F)
      F0=F2
      F2=FH(W1)
      F1=F2
      IF(A.NE.W1) F1=FH(A)
      IF(SIGN(1.,F2).EQ.SIGN(1.,F1)) GO TO 21
      B1=W1
      G=F2
      IF(SIGN(1.,F2).EQ.SIGN(1.,F0)) F=F/2.
      GO TO 20
21    A=W1
      F=F2
      IF(SIGN(1.,F2).EQ.SIGN(1.,F0)) G=G/2.
20    W=W1
      T=(G*A-F*B1)/(G-F)
      RETURN
      END
      FUNCTION FH(T1)
      REAL K,K1(3),L
      COMMON/A4/AZS,ELS,AZ,EL,PI,CONV,RSQ,B,THAZ,THEL,EEL,EAZ,L,TIPL
      COMMON/C1/POS(3),K(3),CAN,SAN,RM,PSN(3),S,C(3),NSKP
      COMMON/F2/K1
      X=POS(1)+T1*K1(1)
      Y=POS(2)+T1*K1(2)
      Z=POS(3)+T1*K1(3)
      FH=SQRT(RSQ-X*X)-B-SQRT(Y*Y+Z*Z)
      RETURN
      END
      SUBROUTINE BNC(VK,VN)
      DIMENSION VK(3),VN(3)
      COMMON/C1/POS(3),K(3),CAN,SAN,RM,PSN(3),S,C(3),NSKP
      DOT=2.*(VN(1)*VK(1)+VN(2)*VK(2)+VN(3)*VK(3))
      C(1)=VK(1)-DOT*VN(1)
      C(2)=VK(2)-DOT*VN(2)
```

```
      C(3)=VK(3)-DOT*VN(3)
      RETURN
      END
      SUBROUTINE THIC(POS,THK)
      DIMENSION POS(3),THK(5)
      THE=ABS(ATAN(POS(3)/POS(2)))
      THK(1)=34.-4.*THE
      THK(1)=(POS(1)-THK(1))/THK(1)
      THK(1)=COS(THK(1)*(.5+ABS((THE-.628)*.108)))
      THK(1)=THK(1)*(.282+.010*THE)*2.54
      RETURN
      END
      SUBROUTINE WALL
      REAL IPD,IPD0,IPD1,K0,LTAN(5),Z(5),U1(5),U2(5),R(5)
      COMMON/B1/NLST,AR(4),AI(4),BR(4),BI(4),CR(4),CI(4)
      COMMON/A1/NLAY,ER(5),LTAN(5)
      COMMON/A2/APAZ,APEL,ILLUM,FREQ,THETA,IPD0,IPD1,RPD0,RPD1
      COMMON/AA2/TRAN0,TRAN1,BKDB,CPHI,SPHI,THK(5)
      NPOL=0
      CTH=COS(THETA)
      STH=SIN(THETA)**2
      K0=0.2094395*FREQ
      MLAY=NLAY+1
 11   NLST=0
      DO 10 I=1,MLAY
      IF(I.NE.(MLAY)) GO TO 12
      Z(I)=1.
      GO TO 13
 12   U1(I)=SQRT(ER(I)-STH)
      Z(I)=CTH/U1(I)
      U2(I)=THK(I)*K0*LTAN(I)/(2.*U1(I))
      U1(I)=U1(I)*K0
      IF(NPOL.EQ.1) Z(I)=1./(ER(I)*Z(I))
      IF(I.NE.1) GO TO 13
      R(1)=(Z(1)-1.)/(Z(1)+1.)
      GO TO 10
 13   R(I)=(Z(I)-Z(I-1))/(Z(I)+Z(I-1))
 10   CONTINUE
      AR(1)=EXP(U2(1))
      AR(4)=1./AR(1)
      AR(2)=R(1)*AR(4)
      AR(3)=R(1)*AR(1)
      AI(1)=U1(1)*THK(1)
      AI(2)=-AI(1)
      AI(3)=AI(1)
      AI(4)=AI(2)
      DO 14 J=2,NLAY
      IF(NLAY.EQ.1) GO TO 40
      BR(1)=EXP(U2(J))
      BR(4)=1./BR(1)
      BR(2)=R(J)*BR(4)
      BR(3)=R(J)*BR(1)
      BI(1)=U1(J)*THK(J)
      BI(2)=-BI(1)
      BI(3)=BI(1)
      BI(4)=BI(2)
      CALL MULT
 14   CONTINUE
 40   CONTINUE
      BR(1)=1.
```

```
      BR(4)=1.
      BR(2)=R(MLAY)
      BR(3)=BR(2)
      BI(1)=0.
      BI(2)=0.
      BI(3)=0.
      BI(4)=0.
      NLST=1
      CALL MULT
      TRAN=1.
      DO 15 K=1,MLAY
15    TRAN=TRAN*(1.-R(K))
      TRAN=TRAN/CR(1)
      SUM=0.
      DO 16 L=1,NLAY
16    SUM=SUM+THK(L)
      IPD=CI(1)-CTH*KO*SUM
      IF(NPOL.EQ.0) GO TO 17
      TRAN1=TRAN
      IPD1=IPD
      RPD1=CI(1)-CI(3)
      RETURN
17    TRANO=TRAN
      IPDO=IPD
      RPDO=CI(1)-CI(3)
      NPOL=1
      GO TO 11
      END
      SUBROUTINE MULT
      COMMON/B1/NLST,AR(4),AI(4),BR(4),BI(4),CR(4),CI(4)
C      COMPLEX MATRIX MULTIPLICATION
      DO 32 N1=1,3,2
      DO 32 N2=1,2
      IF(NLST.EQ.1.AND.N1-N2.EQ.1) RETURN
      R1=AR(N1)*BR(N2)
      R2=AR(N1+1)*BR(N2+2)
      E1=AI(N1)+BI(N2)
      E2=AI(N1+1)+BI(N2+2)
      R3=R1*COS(E1)+R2*COS(E2)
      E3=R1*SIN(E1)+R2*SIN(E2)
      NSET=N2+N1-1
      CR(NSET)=SQRT(R3*R3+E3*E3)
32    CI(NSET)=ATAN2(E3,R3)
      DO 33 I=1,4
      AR(I)=CR(I)
33    AI(I)=CI(I)
      RETURN
      END
```

APPENDIX B.

COMPUTED DATA

The purpose of this Appendix is to document additional data which has been computed during the analysis method validation.

The data presented within the main text of this report has been run for a dielectric constant of 5.0, which is believed to be that of the measured radome article. An increase in dielectric constant to 5.1 resulted in the data shown in Figures B-1 and B-2. Here, there was poorer agreement between theoretical and measured compared to the data in the report.

Secondly, the variation of the distance of the antenna from the base of the radome were tried in an effort to get the crossing points in the measured and computed azimuth scans to match. An antenna to base distance of 17 inches made this agreement fairly good, as seen in Figures B-3 and B-4.

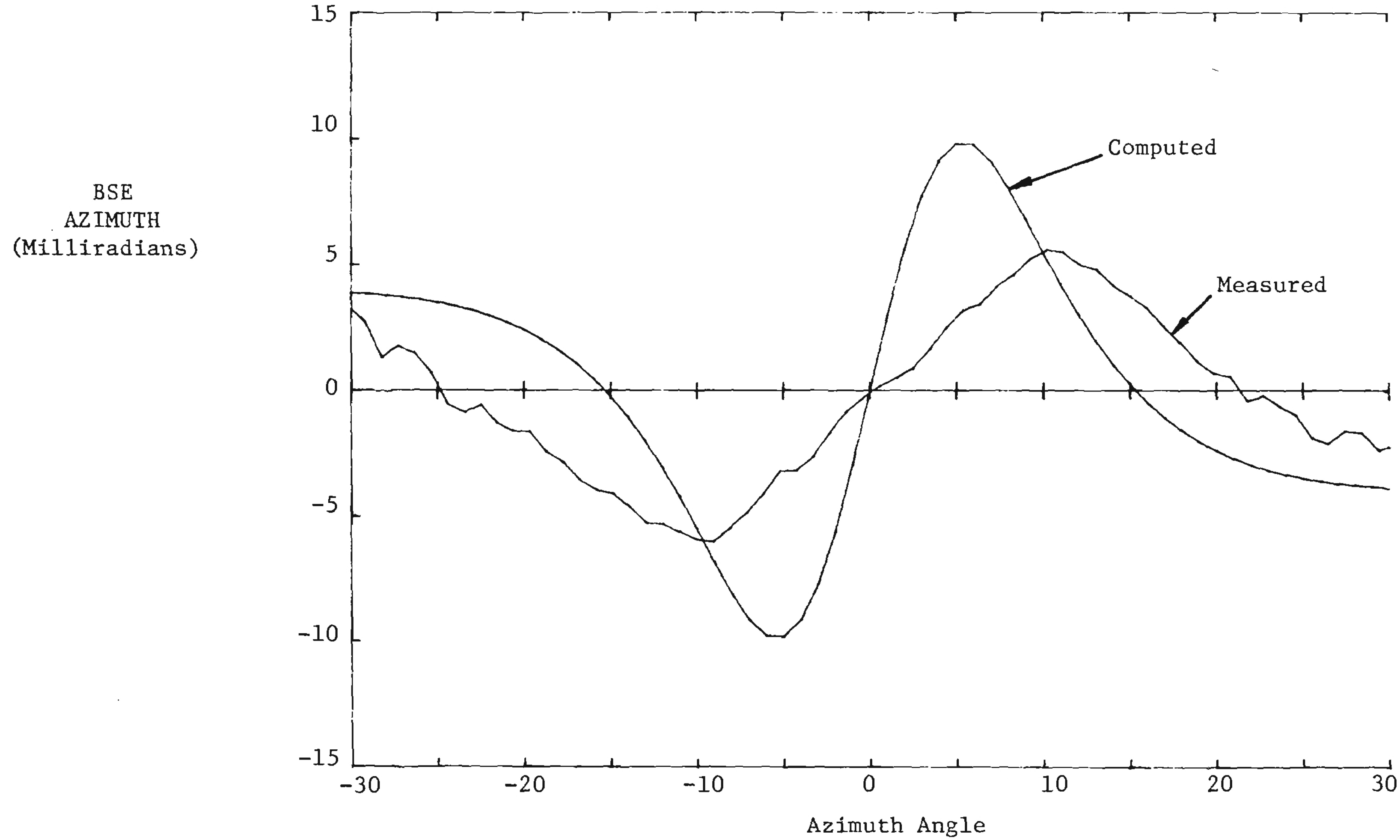

Figure B-1. Azimuth Scan with Dielectric Constant Changed from 5.0 to 5.1

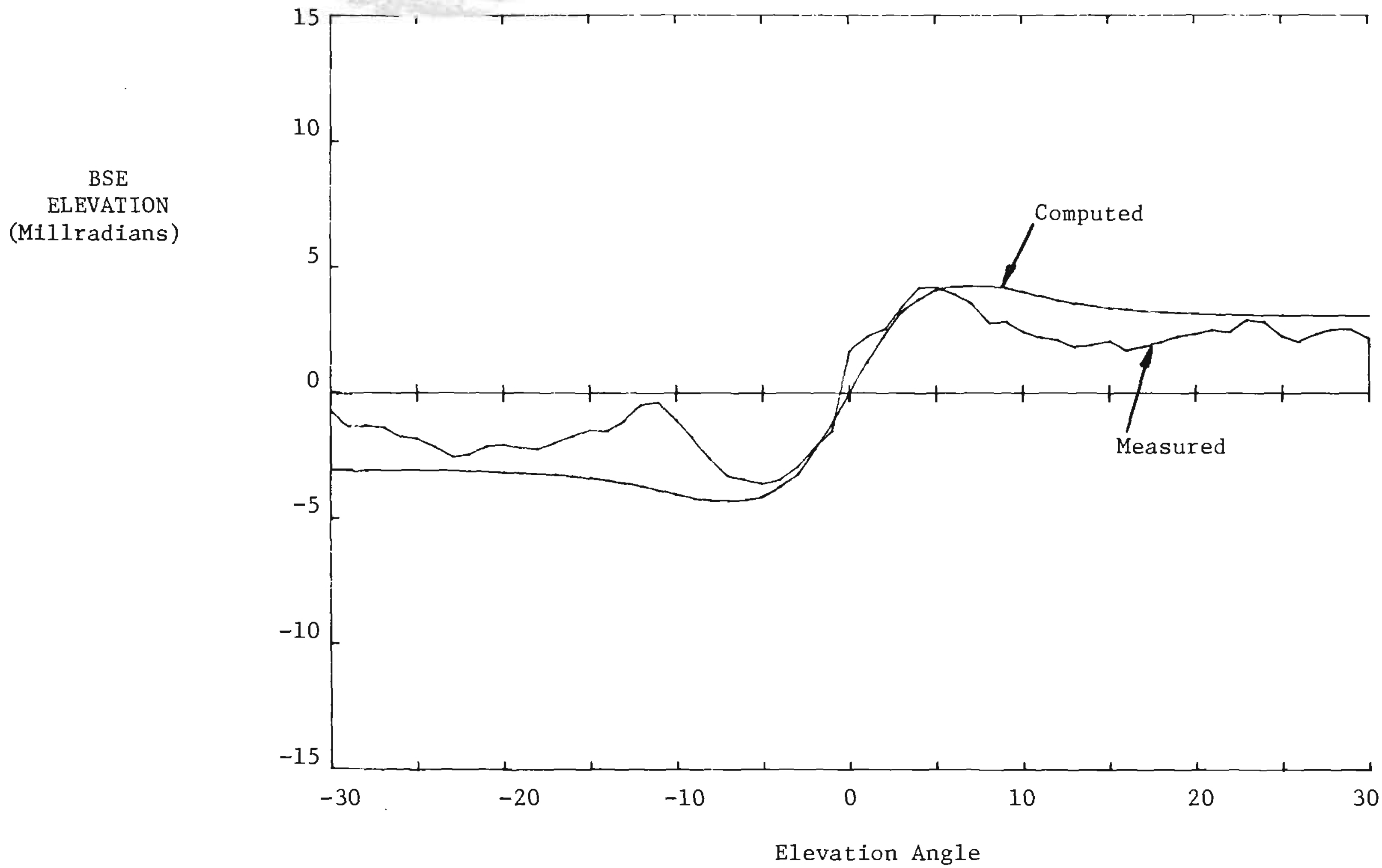

Figure B-2. Elevation Scan with Dielectric Constant Changed from 5.0 to 5.1

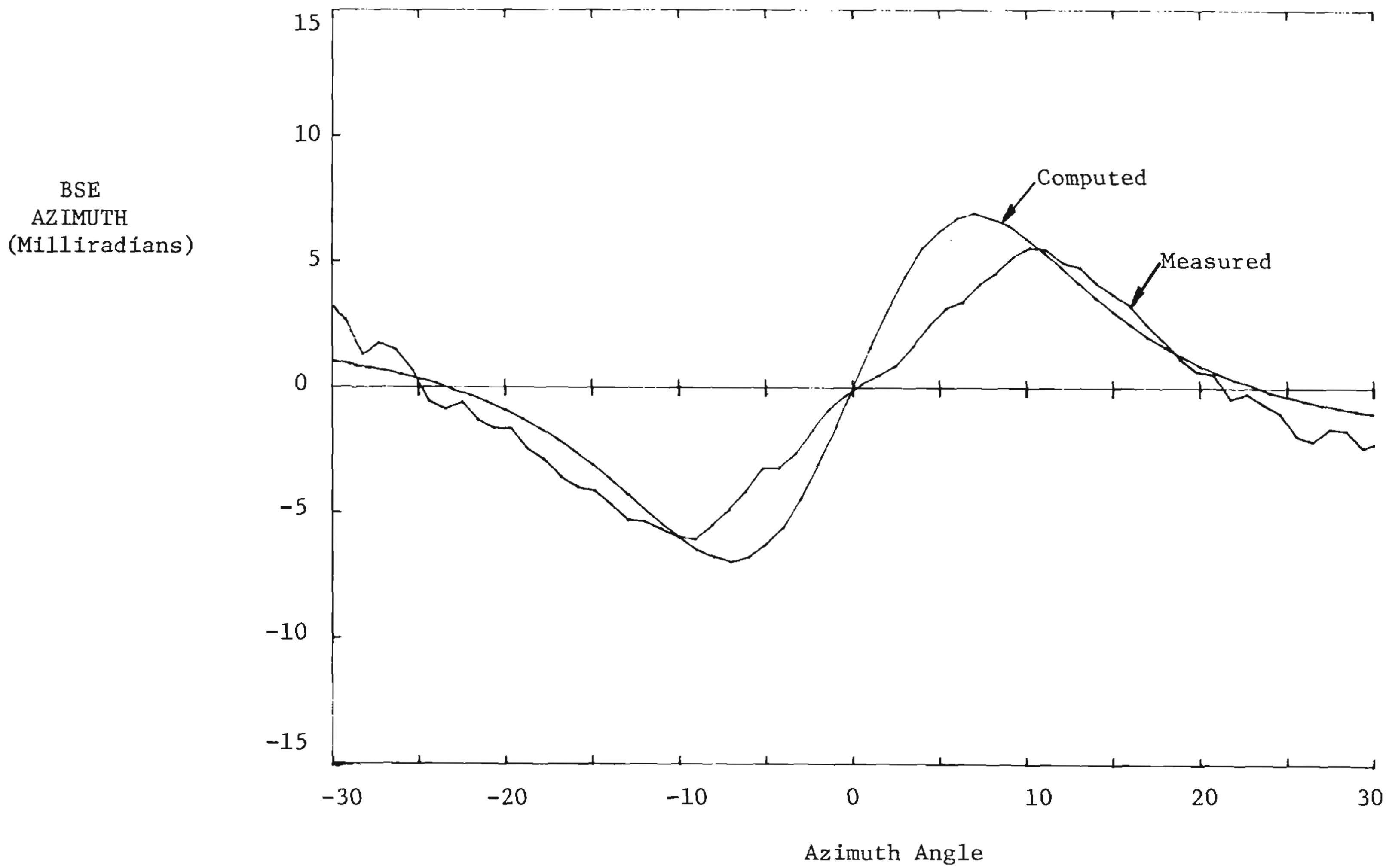

Figure B-3. Azimuth Scan with Antenna's Distance from Base Changed from 10.7 to 17 inches

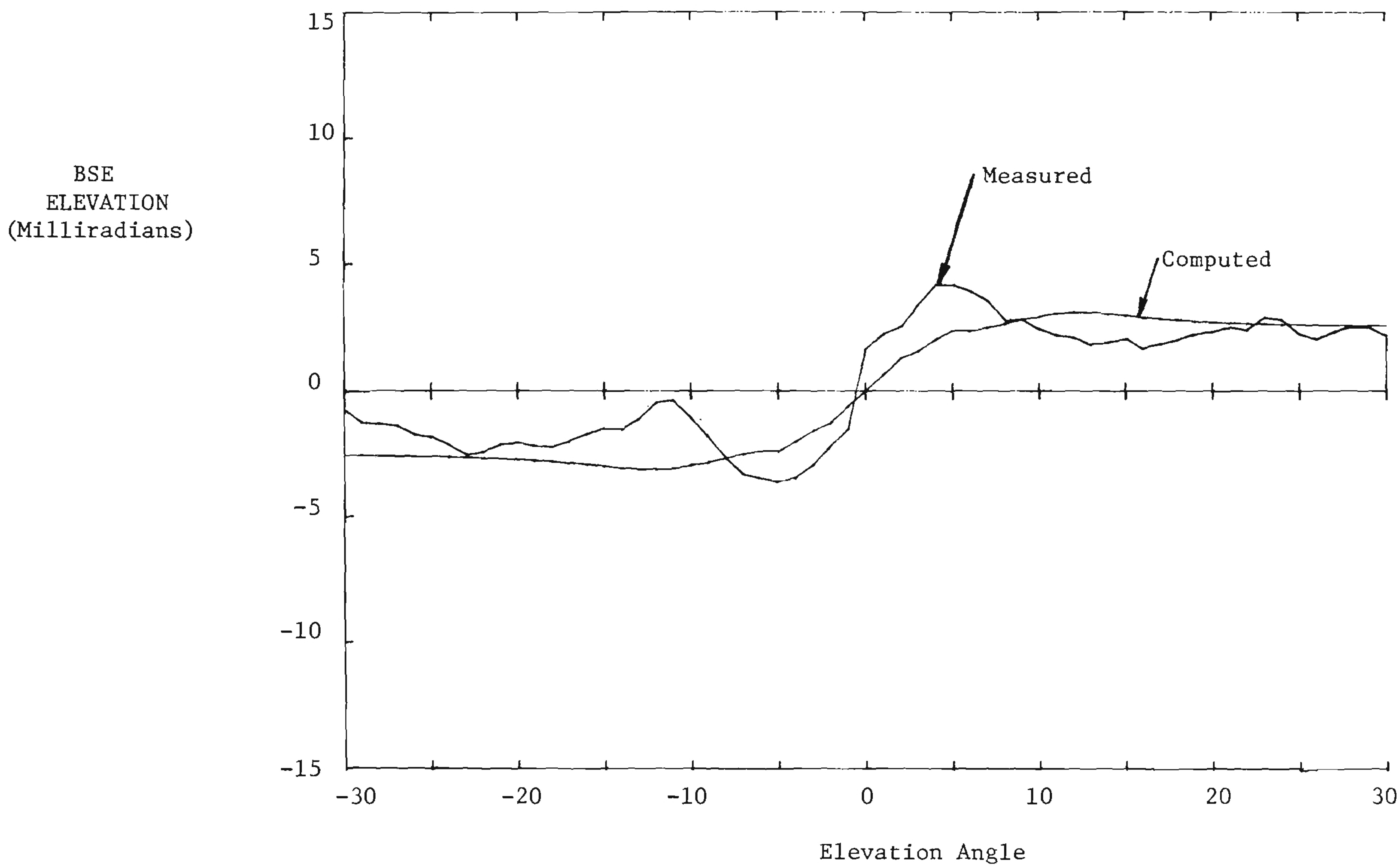

Figure B-4. Elevation Scan with Antenna's Distance from Base Changed from 10.7 to 17 inches.

APPENDIX C

ROTATIONAL MATRIX

The rotational matrix [M] is different for AZ/EL or EL/AZ gimbal configurations. Specifically, for an AZ/EL gimbal

$$[M] = \begin{bmatrix} \cos\theta_{EL} \cos\theta_{AZ} & -\sin\theta_{EL} & \cos\theta_{EL} \sin\theta_{AZ} \\ \sin\theta_{EL} \sin\theta_{AZ} & \cos\theta_{EL} & \sin\theta_{EL} \sin\theta_{AZ} \\ -\sin\theta_{AZ} & 0 & \cos\theta_{AZ} \end{bmatrix} \qquad \text{(A-1)}$$

For an EL/AZ gimbal,

$$[M] = \begin{bmatrix} \cos\theta_{EL} & -\cos\theta_{AZ} \sin\theta_{EL} & \sin\theta_{AZ} \\ \sin\theta_{EL} & \cos\theta_{EL} & 0 \\ -\sin\theta_{AZ} \cos\theta_{EL} & \sin\theta_{EL} \sin\theta_{AZ} & \cos\theta_{AZ} \end{bmatrix} \qquad \text{(A-2)}$$

A unit vector K at the origin in the direction θ is given in terms of the rotational matrices via

$$K = [M] \begin{bmatrix} 1 \\ 0 \\ 0 \end{bmatrix} \qquad \text{(A-3)}$$

At a point y_p, z_p on the antenna face (see Figure A-1), a vector $\overline{P}_1$ from the origin to a point on the antenna (in terms of rotated coordinates) is:

$$P_1 = [M] \begin{bmatrix} 0 \\ y_p \\ z_p \end{bmatrix} \qquad \text{(A-4)}$$

Finally, this is shifted by the distance (x = del) the antenna is offset into the radome.

$$P_2 = P_1 + \begin{bmatrix} del \\ 0 \\ 0 \end{bmatrix} \qquad \text{(A-5)}$$